Bioorganic Chemistry 104 (2020) 104202

Contents lists available at ScienceDirect

Bioorganic Chemistry

journal homepage: www.elsevier.com/locate/bioorg

Synthesis, molecular modeling and antiviral activity of novel 5-fluoro-1*H*-indole-2,3-dione 3-thiosemicarbazones

Zekiye Şeyma Sevinçli[a,b,c,*], Gizem Nur Duran[d], Mehmet Özbil[e], Nilgün Karalı[a]

[a] Department of Pharmaceutical Chemistry, Faculty of Pharmacy, Istanbul University, Istanbul 34116, Turkey
[b] Department of Pharmaceutical Chemistry, Faculty of Pharmacy, Van Yuzuncu Yil University, Van 65080, Turkey
[c] Department of Pharmaceutical Chemistry, Institute of Health Sciences, Istanbul University, Istanbul 34126, Turkey
[d] Chemistry Department, Faculty of Arts and Sciences, Marmara University, Istanbul 34722, Turkey
[e] Department of Biotechnology, Institute of Biotechnology, Gebze Technical University, Kocaeli 41400, Turkey

ARTICLE INFO

Keywords:
Synthesis
Antiviral activity
Thiosemicarbazones
5-Fluoro-1H-indole-2,3-diones
Molecular modeling

ABSTRACT

In this work, novel 5-fluoro-1-methyl/ethyl-1*H*-indole-2,3-dione 3-[4-(substituted phenyl)-thiosemicarbazones] **6a-n** and **7a-n** were synthesized. The antiviral effects of the compounds were tested against HSV-1 (KOS), HSV-2 (G) HSV-1 TK$^-$ KOS ACV^r and VV in HEL cell cultures using acyclovir and ganciclovir as standards, and Coxsackie B4 virus in Vero cell cultures using ribavirin and mycophenolic acid as standards. R_2 ethyl substituted **7** derivatives were found effective against viruses tested. R_1 4-CF_3 substituted **7d**, R_1 4-OCH_3 substituted **7 g** and R_1 3-Cl substituted **7 l** showed activity against HSV-1 (KOS), HSV-2 (G) HSV-1 TK$^-$ KOS ACV^r and VV. Whereas only R_1 4-Br substituted **7n** has selective activity against coxsackie B4 virus. Molecular modeling studies of **7d** and **7l** were performed to determine binding side on HSV-1 glycoprotein B and D, HSV-2 glycoprotein B structures.

1. Introduction

1*H*-Indole-2,3-dione (isatin) and its derivatives have a broad spectrum of biological properties including antituberculosis, antiviral and anticancer activities. There are several reports on antiviral activities of 1*H*-indole-2,3-dione 3-thiosemicarbazone derivatives [1–3]. Methisazone (*N*-methylisatin 3-thiosemicarbazone), synthesized for the vaccinia virus causing smallpox, is the first derivative of isatin 3-thiosemicarbazone [4,5]. Herpes simplex virus-1 (HSV-1), which is a member of the HSV family and acquired mainly in young ages, causes infections in the upper half of the body, while herpes simplex virus-2 (HSV-2) causes genital infections through sexual contact [6,7]. It has been determined that thiocarbonyl group is essential for antiherpetic activity against HSV-1, HSV-2 and the presence of a 4-substituted phenyl ring at the N4 position of thiosemicarbazone increases antiviral activity [8,9]. Coxsackie viruses are enteroviruses of the *Picornaviridae* family which are classified as group A and group B. Coxsackie virus group B, which has six members, causes childhood myocarditis, cardiomyopathy, diabetes and neurological disorders [10]. There are many reports showing that Coxsackie B4 virus causes type 1 diabetes by damaging β-cells in the pancreas [11–13]. There are studies in the literature on the effect of thiosemicarbazones on coxsackie B4 virus [14,15]. In 2013, Abbas and co-workers found that 5-fluoroisatin 3-thiosemicarbazone derivatives inhibit viral replication [3].

In the present study, 5-fluoro-1-methyl/ ethyl-1*H*-indole-2,3-dione 3-[4-(substituted phenyl)thiosemicarbazone] derivatives **6a-n** and **7a-n** were synthesized by reaction of 4-(substituted phenyl)thiosemicarbazid derivatives **2a-n** with 5-fluoro-1-methyl/ethyl-1*H*-indole-2,3-dione **4**/**5**. The structures of all the synthesized compounds were determined by analytical and spectral methods. The molecular and isomeric structures of **6h** and **6j** were determined by X-ray single crystal diffraction analysis [16,17]. Antiviral activities of **6a-n** and **7a-n** were evaluated against HSV-1 (KOS), HSV-2 (G) HSV-1 TK$^-$ KOS strain resistant to acyclovir (ACV^r) and VV in HEL cell (human embryonic lung fibroblast cell) cultures, and Coxsackie B4 virus in Vero cell (African green monkey kidney cell) cultures. Molecular modeling studies of **7d** and **7l** were completed on HSV-1 glycoprotein B (gB), HSV-1 glycoprotein D (gD), and HSV-2 (gD) protein structures.

Abbreviations: HSV-1 (KOS), herpes simplex virus-1 (strain KOS); HSV-1 TK$^-$ KOS ACV^r, herpes simplex virus-1 (TK$^-$ KOS strain resistant to acyclovir); HSV-2, herpes simplex virus-2 (strain G); VV, vaccinia virus; gB, glycoprotein B; gD, glycoprotein D; EC_{50}, 50% effective concentration; MCC, minimum inhibitory concentration; HEL cell, human embryonic lung fibroblast cell; Vero cell, African green monkey kidney cell

* Corresponding author at: Department of Pharmaceutical Chemistry, Van Yuzuncu Yil University, 65080 Van, Turkey.
E-mail address: seymasevincli@yyu.edu.tr (Z.Ş. Sevinçli).

https://doi.org/10.1016/j.bioorg.2020.104202
Received 8 June 2020; Received in revised form 11 August 2020; Accepted 18 August 2020
Available online 26 August 2020

Table 1
Substituents and substituent positions of **6a-n** and **7a-n.**

Compound	R_1	R_2	Compound	R_1	R_2
6a	H	CH_3	**7a**	H	C_2H_5
6b	3-CH_3	CH_3	**7b**	3-CH_3	C_2H_5
6c	4-CH_3	CH_3	**7c**	4-CH_3	C_2H_5
6d	4-CF_3	CH_3	**7d**	4-CF_3	C_2H_5
6e	4-C_2H_5	CH_3	**7e**	4-C_2H_5	C_2H_5
6f	3-OCH_3	CH_3	**7f**	3-OCH_3	C_2H_5
6g	4-OCH_3	CH_3	**7g**	4-OCH_3	C_2H_5
6h	4-SCH_3	CH_3	**7h**	4-SCH_3	C_2H_5
6i	4-OCF_3	CH_3	**7i**	4-OCF_3	C_2H_5
6j	3-F	CH_3	**7j**	3-F	C_2H_5
6k	4-F	CH_3	**7k**	4-F	C_2H_5
6l	3-Cl	CH_3	**7l**	3-Cl	C_2H_5
6m	4-Cl	CH_3	**7m**	4-Cl	C_2H_5
6n	4-Br	CH_3	**7n**	4-Br	C_2H_5

2. Results and Discussion

2.1. Chemistry

In this study, hydrazine hydrate was reacted with substituted phenyl isothiocyanates **1a-n** in ethanol to give 4-(substituted phenyl)thiosemicarbazides **2a-n**. A suspension of 5-fluoro-1*H*-indole-2,3-dione **3** potassium carbonate (K_2CO_3) and potassium iodide (KI) in anhydrous N,*N*-dimethylformamide (DMF) was added iodomethane (CH_3I)/ bromoethane (C_2H_5Br) to yield 5-fluoro-1-methyl/ethyl-1*H*-indole-2,3-dione **4**/**5**. A series of 5-fluoro-1-methyl/ethyl-1H-indole-2,3-dione 3-[4-(substituted phenyl) thiosemicarbazones] **6a-n** and **7a-n** (Table 1) were synthesized by reacting **2a-n** with 5-fluoro-1-methyl/ethyl-1H-indole-2,3-dione **4**/**5** in ethanol. A catalytic amount of sulfuric acid (H_2SO_4) was added to the reaction to synthesize **6a**, **6b**, **6d**, **6e**, **6 l**, **7a** and **7b**. The structures of **6a-n** and **7a-n** were confirmed by analytical and spectral (IR, ^{1}H NMR, ^{13}C NMR, HSQC-2D, HMBC-2D, HRMS-ESI+ and LCMS-ESI+) data (Scheme 1).

IR spectra of **6a-n** and **7a-n** showed two or three separate absorption bands in the 3354–3196 cm^{-1} region resulting from the NH stretchings of the thioamide groups. The aromatic = C−H C=N stretching band, aromatic C=C stretching and N−H bending combination band were identified at 3101–3010 and 1625–1473 cm^{-1} regions, respectively. The lactam C=O and thioamide C=S stretchings were observed at 1674–1701 and 1253–1278 cm^{-1} regions, respectively.

^{1}H NMR spectra of **6a-n** and **7a-n** displayed the thioamide N_4 and N_2 protons of the thiosemicarbazone moiety as two separate singlets at δ 10.73–11.00 and 12.55–12.73 ppm regions, respectively. The exchangeable NH proton signals were further confirmed by deuterium oxide (D_2O) exchange experiments of **6c** and **7l**. Observation of the methyl signals in the spectra of **6a-n**, methyl and methylene signals in the spectra of **7a-n** proved 1-alkylation while the lactam NH signal of the 2-indolinone ring was not observed in the spectra. 2-Indolinone and phenyl ring proton resonances of new compounds were found in the expected regions with appropriate coupling constants and integral values. The ^{1}H NMR spectra of **6a-n** and **7a-n**, indole C_4-H usually was observed at δ 7.63–7.69 ppm as doublet of doublet making the ortho coupling with fluorine and meta coupling with the indol C_6-H. At δ 7.59–7.68, indole C_4-H gave a multiplet signals with phenyl protons in **6j**, **6l**, **6m**, **7l** and **7m**. The indole C_6-H usually signaled at δ 7.27–7.30 ppm as triplet of doublet making meta coupling with the indol C_4-H and ortho coupling with fluorine and indol C_7-H. At δ 7.20–7.35, indole C_6-H gave a multiplet signals with phenyl protons or indole C_7-H in **6a**, **6b**, **6e**, **6f**, **6h**, **6k**, **6l**, **7a**, **7b**, **7e**, **7f**, **7h** and **7k**. The indole C_7-H signaled at δ 7.14–7.16 ppm as doublet of doublet in **6a-n** making the meta coupling with fluorine and ortho coupling with the indol C_6-H. The indole C_7-H in **7a-n** generally was observed at δ 7.21–7.24 ppm as doublet of doublet whereas it was signaled at δ 7.20–7.23 ppm with phenyl $C_{3,5}$-H in **7c** and δ 7.20–7.34 ppm with indole C_6-H and phenyl protons as multiplet in **7f** and **7k**.

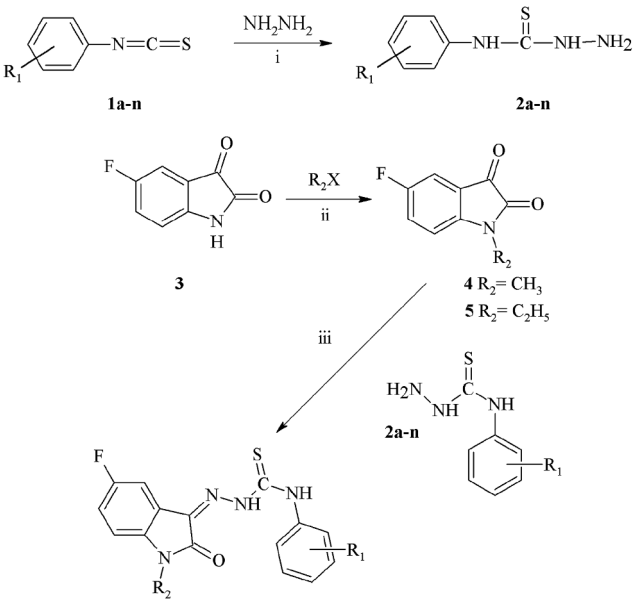

Scheme 1. Synthesis of **6a-n** and **7a-n**. Reagents and conditions: i) Ethanol, stirred, cooled ii) K_2CO_3, KI, DMF, CH_3I/ C_2H_5Br, strirred, reflux iii) Ethanol or ethanol and H_2SO_4, reflux.

^{13}C NMR-decoupled run on **6a-d**, **6f, 6g, 6i-l**, **6n**, **7c-e, 7g-n** and ^{1}H–^{13}C cross correlation run on **6e**, **6h**, **6m**, **7a**, **7b** and **7f** allowed the complete assignment of the proton and carbon NMR signals. The resonances of indole C_3, indole C_2 and C=S were detected at δ 130.70–131.76, 160.73–161.40 and 175.62–177.23 ppm, respectively. Fluorine substituted indole C_5 signal was observed at δ 159.03–159.32 ppm as doublet (J = 238–242 Hz). Mass spectra of **6a-d**, **6f, 6g, 6i**, **6k-n**, **6n**, **7b-n** were taken by Electrospray Ionization positive ionization method (ESI+). In the spectra $[M+H]^+$ peaks were observed which confirmed their molecular weights. The molecular and isomeric structures of **6h** and **6j** were determined by X-ray single crystal diffraction analysis and the stable isomer was found to be in Z configuration (Figs. 1 and 2) [16,17].

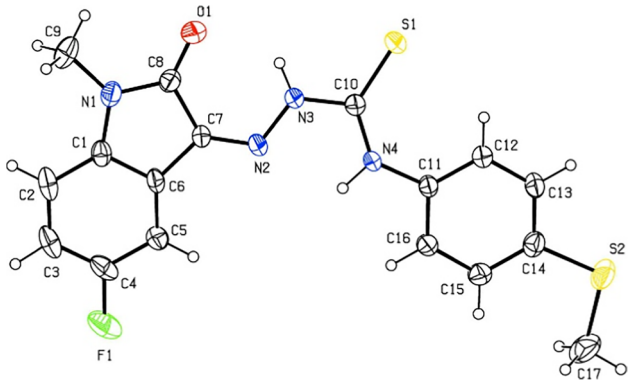

Fig. 1. View of the molecular structure of **6h**, with the atom labelling[16.]

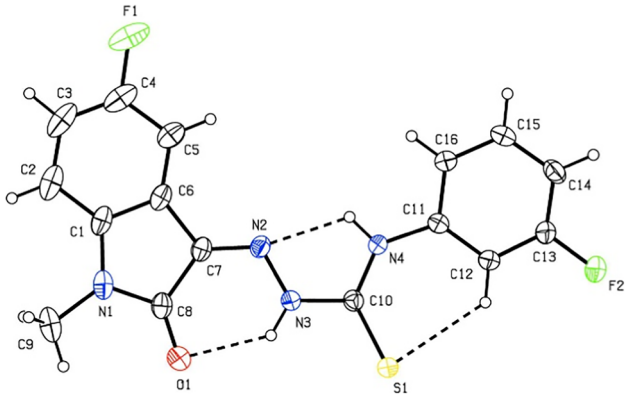

Fig. 2. View of the molecular structure of **6j**, with the atom labelling[17].

2.2. Antiviral Activity

The antiviral effects of the compounds were tested against HSV-1 (KOS), HSV-2 (G), HSV-1 TK$^-$ KOS ACV^r and VV in HEL cell cultures, Coxsackie B4 virus in Vero cell cultures. For all derivatives, the 50% effective concentration (EC_{50}) and minimum cytotoxic concentration (MCC) were determined. R_2 ethyl substituted **7d**, **7g** and **7l** were effective and nontoxic against HSV-1 (KOS), HSV-2 (G), HSV-1 TK$^-$ KOS ACV^r and VV at low μM doses. **7n** showed antiviral effect against Coxsackie B4 virus at 10 μM. The most effective **7** derivative against HSV-1 and HSV-2 strains was found to be R_1 4-CF_3 substituted **7d**. The compound is effective at 6.8, 7.6 and 2.3 μM against HSV-1 (KOS), HSV-2 (G) and HSV-1 TK$^-$ KOS ACV^r, respectively. While R_1 4-Cl substituted **7m** and R_1 3-F substituted **7j** are inactive and toxic, R_1 3-Cl substituted **7l** was found to be nontoxic and effective at 6.8, 8.9 and 6.8 μM against HSV-1 (KOS), HSV-2 (G) and HSV-1 TK$^-$ KOS ACV^r, respectively. Whereas R_1 3-OCH_3 substituted **7f** is inactive against all viruses tested. R_1 4-OCH_3 substituted **7g** is active against HSV-1 (KOS), HSV-2 (G) and HSV-1 TK$^-$ KOS ACV^r at 20 μM. **7d**, **7g** and **7l** were found to be high effective against HSV-2 (G) and HSV-1 TK$^-$ KOS ACV^r compared to brivudine and also **7d** was determined more active against HSV-1 TK$^-$ KOS ACV^r compared to acyclovir. **7d** and **7l** were found to be high effective against VV compared to brivudin, acyclovir and ganciclovir at 8.9 μM whereas **7g** was determined more active compared to acyclovir and ganciclovir at 45 μM. Only R_1 4-Br substituted **7n** had selective effect at 10 μM against Coxsackie B4 virus in tested compounds (Tables 2 and 3). The test results show the importance of the ethyl group in position 1 of the indole ring and the electron-attracting groups as 4-CF_3, 4-OCH_3, 3-Cl and 4-Br in the phenyl ring of the thiosemicarbazone residue for antiviral effect. Whereas, the R_2 methyl substituted **6** derivatives were found to be inactive against all viruses tested (Table S1-S2). Based on these results, more effective 5-fluoro-1-ethyl-2-indolinone derivatives can be designed and synthesis.

2.3. Molecular Modeling

Binding of compounds **7d** and **7l** on HSV-1 (gB), HSV-1 (gD), and HSV-2 (gD) were evaluated computationally. Lack of 3D structure of HSV-2 (gB) protein restrained the full comparison. However comparisons between two different proteins from the same virus (HSV-1) and the same protein (gD) from two different types of viruses (HSV-1 and HSV-2) could be made.

2.3.1. HSV-1 (gB)

Molecular docking simulations of **7d** to HSV-1 glycoprotein B (gB) produced the binding pose in Fig. 3. The ligand was bound to the binding site formed by amino acids Tyr 301, Arg 304, Ser 307, Gln 321, Thr 341, Asn 343, Trp 356, Lys 359. These interactions are listed in Table 4. The binding pocket consisted of polar residues, thus, ligand was bound through mostly hydrogen bonds (H-bonds). Moreover, Tyr 301 creates a halogen bond with F atom of the ligand and Trp 356 creates π-stacking with the ligand. The binding affinity of the ligand was calculated as −7.9 kcal/mol.

Ligand **7l** was bound to the binding site formed by amino acids Gly 302, Arg 304, Gln 321, Thr 340, Thr 341, and Trp 356, which is very similar to the binding site of ligand **7d** (Fig. 3).

Due to bulky and polar CF_3 group, compared to smaller Cl group, the orientation of **7l** shifted towards outwards of the protein. Trp 356 and Gly 302 create two small hydrophobic clefts and number of H-bonds formed between protein and ligands decreased in the case of ligand **7l** (Table 4). Thus, the binding affinity of the ligand was calculated as −7.4 kcal/mol, 0.5 kcal/mol lower than that of ligand **7d**.

2.3.2. HSV-1 (gD)

HSV-1 (gD) was modeled as a homodimer according to its biological assembly. Compound **7d** bound to HSV-1 (gD) protein right at the interface of two monomers. The the binding site formed by amino acids by Asp 139*, Ser 140*, Leu 139, Pro 194, Tyr 234, Ser 235, Ser 235*, and Ile 238 (Fig. 4). The ligand interacted through H-bonds with amino acids Asp 139*, Pro 194, and Ser 235. It also created hydrophobic interactions with Ser 140*, Leu 193, Tyr 234, Ser 235*, and Ile 238. These interactions are listed in Table 4. The binding affinity of compound **7d** was calculated as −7.3 kcal/mol at this binding site. The positioning of compound **7d** might be very critical for disrupting the assembly of homodimer HSV-1 gD protein.

Ligand **7l** was bound to the binding site formed by amino acids Ser 68, Leu 70, Glu 146, Leu 152, His 154, Val 233, Trp 241, Gly 243, Pro 244, Ala 246, and Pro 247. This binding site was highly non-polar. Thus, the ligand was embedded inside the protein, forming mainly hydrophobic interactions. Moreover, Ser 68 creates a H-bond with O atom of the ligand and Gly 243 creates H-bond with N of the ligand. The binding affinity of the ligand was calculated as −7.2 kcal/mol.

2.3.3. HSV-2 (gD)

Molecular docking simulations were only performed on HSV-2 (gD) protein as there is no 3-D structure of HSV-2 (gB) protein available. Upon molecular docking to HSV-2 (gD) protein, Ligand **7d** was bound to the binding site formed by amino acids Ser 52, Ile 80, Ala 88, Tyr 120, Ile 170, Asp 172, Trp 173 (Fig. 5). The binding site was formed by both polar and mostly non-polar amino acids. The ligand interacted through H-bonds with amino acids Ser 52, Tyr 120, and Asp 172. Two H-bonds were formed between Ser 52 and CF_3 group of the ligand. It also created π-stacking with Trp 173. Ile 80, Ala 88, and Ile 170 formed hydrophobic clefts, where indole group fitted in. The binding affinity of the ligand was calculated as −7.4 kcal/mol.

Ligand **7l** was bound to the binding site formed by amino acids Pro 51, Ile 53, Thr 56, Tyr 58, Pro 74, Glu 76, Glu 175, Ile 176, Thr 177, and Leu 252. This binding pocket was buried inside the protein, compared to binding pocket for ligand **7d**. The ligand interacted with the protein mainly through H-bonds from residues Thr 56, Tyr 58, and Thr 177. It also created hydrophobic interactions with Pro 51, Ile 53, Pro 74, sidechain ethyl groups of Glu 76, and Leu 252 amino acids. The Cl group created strong H-bond with backbone amine H atom of Leu 252. Moreover, indole group interacted with glutamate ion of Glu 175 through π-anion interaction and F group with Ile 176 through halogen bond (Table 6).

The binding affinity of the ligand was calculated as −7.5 kcal/mol, 0.1 kcal/mol higher than that of ligand **7d**. Main reason for this slight increment was the more buried ligand position for ligand **7l** inside the protein, thus increased number of interactions.

When binding affinities of compounds **7d** and **7l** are compared on the same virus, HSV-1, it was clear that binding affinities were higher for gB protein than they were for gD protein (Tables 4 and 5). Binding affinity for compound **7d** on HSV-1 (gB) protein was calculated as −7.9 kcal/mol, which was the highest binding affinity in this study. The binding affinity comparison for compounds **7d** and **7l** for the same

Table 2
Antiviral activities of **7** derivatives against HSV-1 (KOS), HSV-2 (G) HSV-1 TK$^-$ KOS ACV^r and VV in HEL cell cultures.

Compound	R_1	R_2	MCC	EC_{50} (μM)			
				HSV-1 (KOS)	HSV-2 (G)	HSV-1 TK$^-$KOS ACV^r	VV
7a	H	C_2H_5	≥50	> 50	> 50	> 50	> 50
7j	3-F	C_2H_5	> 50	> 50	> 50	> 50	> 50
Brivudin			> 250	0.03	146	250	100
Acyclovir			> 250	0.2	0.9	113	> 250
Ganciclovir			> 100	0.01	0.02	0.03	> 100
7b	3-CH_3	C_2H_5	> 100	> 100	> 100	> 100	> 100
7c	4-CH_3	C_2H_5	> 100	> 100	> 100	> 100	> 100
7d (test 1)	4-CF_3	C_2H_5	≥20	**7.6**	**7.6**	**4**	**12**
(test 2)			100	**6.8**	**8.9**	**2.3**	**8.9**
7e	4-C_2H_5	C_2H_5	≥100	> 100	> 100	> 100	> 100
7f	3-OCH_3	C_2H_5	≥100	> 100	> 100	> 100	> 100
7h	4-SCH_3	C_2H_5	100	> 100	> 100	> 100	> 100
7i	4-OCF_3	C_2H_5	≥20	> 100	> 100	> 100	> 100
7l (test 1)	3-Cl	C_2H_5	> 100	**8.9**	**12**	**7.6**	**10**
(test 2)			100	**6.8**	**8.9**	**6.8**	**8.9**
Brivudin			> 250	0.08	> 250	250	22
Acyclovir			> 250	3.8	0.29	3.5	> 250
Ganciclovir			> 100	0.11	0.3	0.35	> 100
7g (test 1)	4-OCH_3	C_2H_5	100	> 100	**20**	**20**	> 100
(test 2)			> 100	**20**	**34**	**50**	**45**
7k	4-F	C_2H_5	4	> 100	> 100	> 100	> 100
7m	4-Cl	C_2H_5	≥4	> 100	> 100	> 100	> 100
7n	4-Br	C_2H_5	≥4	> 100	> 100	> 100	> 100
Brivudin			> 250	0.04	50	50	22
Acyclovir			> 250	0.2	0.2	85	> 250
Ganciclovir			> 100	0.032	0.06	8.9	> 100

[a]EC_{50}: 50% effective concentration, producing 50% inhibition of virus-induced cytopathic effect, as determined by microscopy.
[b]MCC: minimum inhibitory concentration, or compound concentration causing minimal changes in cell morphology, as assessed by microscopy.

Table 3
Antiviral activities of **7** derivatives against Coxsackie B4 virus in Vero cell cultures.

Compound	R_1	R_2	MCC	EC_{50} (μM) Coxsackie B4 virus
7a	H	C_2H_5	> 50	> 50
7b	3-CH_3	C_2H_5	≥20	> 100
7c	4-CH_3	C_2H_5	≥4	> 100
7d	4-CF_3	C_2H_5	≥4	> 100
7e	4-C_2H_5	C_2H_5	≥4	> 100
7f	3-OCH_3	C_2H_5	4	> 100
7h	4-SCH_3	C_2H_5	20	> 100
7i	4-OCF_3	C_2H_5	≥4	> 100
7j	3-F	C_2H_5	≥10	> 50
7l	3-Cl	C_2H_5	4	> 100
DS-10.000 (μg/ml)			> 100	8.9
Ribavirin			> 250	> 250
Mycophenolic acid			> 100	> 100
7g	4-OCH_3	C_2H_5	100	> 100
7k	4-F	C_2H_5	≥100	> 100
7m	4-Cl	C_2H_5	≥100	> 100
7n (test 1)	4-Br	C_2H_5	≥100	**10**
(test 2)			100	**10**
DS-10.000 (μg/ml)			> 100	1.8
Ribavirin			≥250	> 250
Mycophenolic acid			> 100	> 100

gD protein for HSV-1 and HSV-2 yielded very similar affinities. Affinities were very similar between −7.2 and −7.5 for both proteins. However, for HSV-1 (gD) protein compound **7d** was binding slightly better than compound **7l**, but for HSV-2 (gD) protein compound **7l** was calculated to bind slightly better than compound **7d** (Tables 5 and 6).

3. Conclusions

In summary, while the ethylated derivatives were determined to be active, no activity was observed in the methyl derivatives. **7d, 7l** and **7g** were found to be effective against HSV-1 (KOS), HSV-2 (G), HSV-1 TK$^-$ KOS ACV^r and VV at low micromolar levels, while **7n** showed antiviral effect against Coxsackie B4 virus at 10 μM. Molecular docking simulations were performed for **7d** and **7l** on HSV-1 (gB), HSV-1 (gD), and HSV-2 (gD). The binding affinities of the **7d** were calculated as −7.9, −7.3 and −7.4 kcal/mol on HSV-1 (gB), HSV-1 (gD), and HSV-2 (gD) respectively, while for **7l** were calculated as −7.4, −7.2 and −7.5 kcal/mol on HSV-1 (gB), HSV-1 (gD), and HSV-2 (gD).

4. Experimental protocols

4.1. Chemistry

Melting points were estimated with a Buchi 540 melting point apparatus in open capillaries and are uncorrected. Elemental analyses were performed on a Thermo Finnigan Flash EA 1112 elemental analyzer. IR spectra were recorded on KBr discs, using a Shimadzu IRAffinity-1 FTIR spectrometer. ^{1}H NMR, ^{13}C NMR, HSQC-2D and HMBC-2D spectra were obtained on VarianUNITY INOVA 500, Varian Mercury (Agilent) 400 and Varian Mercury 300 NMR spectrophotometers using DMSO-d_6. HRMS and LC/MS datas were recorded by Thermo Scientific, TSQ-Quantum Access and Waters 2695 Alliance Micromass ZQ LC/MS, respectively.

4.1.1. The synthesis of 4-(substituted phenyl) thiosemicarbazides (2a-n)

To a solution of hydrazine hydrate (5 mmol) in ethanol (10 mL), a suspension of (substituted phenyl)isothiocyanates **1a-n** (5 mmol) in ethanol (10 mL) was added dropwise with vigorous stirring and cooling in an ice bath. The mixture was allowed to stand overnight. The obtained solid molecules were filtered, washed three times with water (30 mL), dried, recrystallized from ethanol. The structures of **2a-n** in the literature were confirmed by analytical and spectral data by researcher except **2e** [18–22].

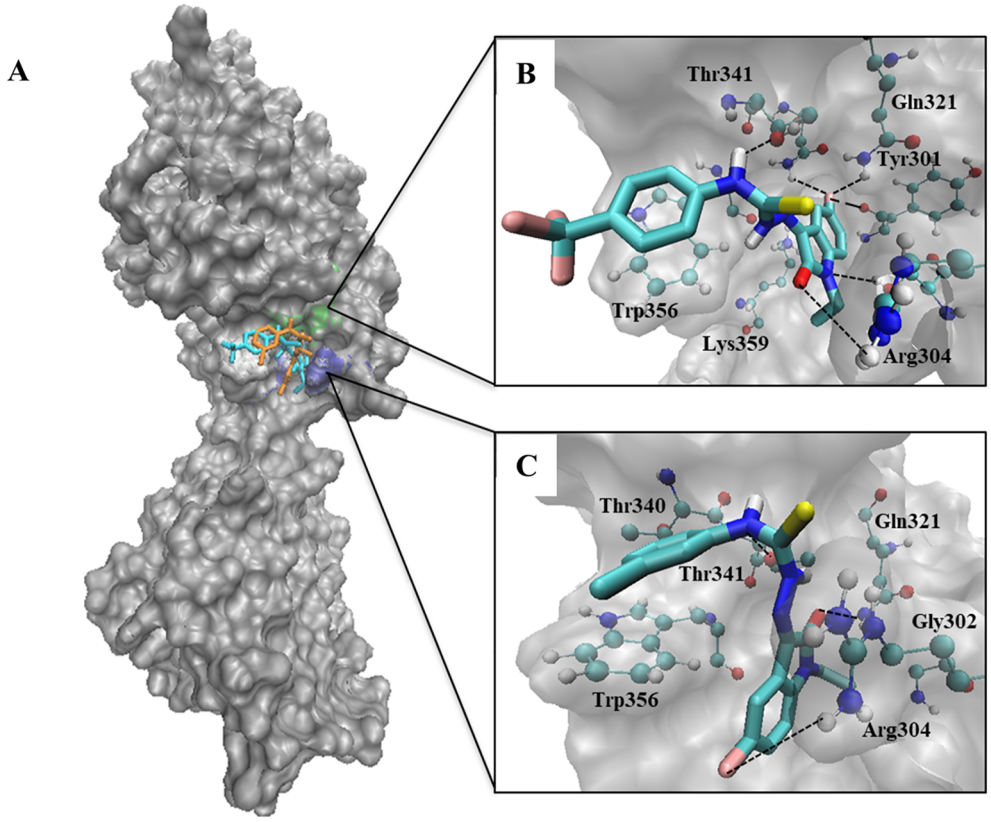

Fig. 3. A) Docking poses for compound **7d** in cyan, **7l** in orange, on HSV-1 (gB) protein. Polar residues were shown in green, basic residues in blue, and hydrophobic residues in white. **B)** Zoomed in view of ligand **7d**. **C)** Zoomed in view of ligand **7l**. (For interpretation of the references to colour in this figure legend, the reader is referred to the web version of this article.)

Table 4
Binding pockets on HSV-1 (gB) protein.

Compound	Interacting Amino Acids	Interaction Types	Binding Affinity (kcal/mol)
7d	Tyr 301	Halogen Bond	**−7.9**
	Arg 304	H-Bond	
	Ser 307	H-Bond	
	Gln 321	H-Bond	
	Thr 341	H-Bond	
	Asn 343	H-Bond	
	Trp 356	π-Stacking	
	Lys 359	H-bond	
7l	Gly 302	Hydrophobic	**−7.4**
	Arg 304	H-Bond	
	Gln 321	H-Bond	
	Thr 340	H-Bond	
	Thr 341	Hydrophobic	
	Trp 356	π-Stacking	

4.1.2. 4-(4-Ethylphenyl)thiosemicarbazide (2e)

White powder (88%): mp 133–135 °C; IR (KBr): υ 3340, 3277, 3190 (NH), 1278 (C—N), 1207 (C=S). ^{1}H NMR (DMSO-d_6/ 300 MHz) ppm: 0.97 (3H, t, J: 7.6 Hz, CH_2CH_3), 2.37 (2H, q, J: 7.6 Hz, CH_2CH_3), 4.56 (2H, s, NH_2), 6.92–6.98 (2H, m, AA′BB′ system phenyl $C_{3,5}$-H), 7.21–7.31 (2H, m, AA′BB′ system, phenyl $C_{2,6}$-H), 8.85 (1H, s, N_4-H), 9.40 (1H, s, N_2-H). ^{13}C NMR (DECOUPLED DMSO-d_6/ 75 MHz): 16.00 (CH_3), 27.89 (CH_2), 124.03 (phenyl $C_{2,6}$), 127.58 (phenyl $C_{3,5}$), 137.07 (phenyl C_1), 139.93 (phenyl C_4), 179.63 (C=S).

4.1.3. The synthesis of 5-fluoro-1-methyl/ ethyl-1H-indole-2,3-dione (4 and 5)

A suspension of 5-fluoro-1*H*-indole-2,3-dione **3** (5 mmol), K_2CO_3 (7 mmol) and KI (1 mmol) in anhydrous DMF (5 mL) was stirred for 30 min at room temperature. After addition of CH_3I or C_2H_5Br (15 mmol), the mixture was heated at 50 °C for 4 h. Completion of the reaction was controlled with TLC method. The product was poured onto ice–water. The solid molecules formed were filtered, dried, recrystallized from ethanol. The structures of **4** and **5** in the literature were confirmed by analytical and spectral data by researcher [23–25].

4.1.4. The synthesis of 5-fluoro-1-methyl/ ethyl-1H-indole-2,3-dione 3-[4-(substituted phenyl) thiosemicarbazone] derivatives (6a-n and 7a-n)

4-(Substituted phenyl) thiosemicarbazides (**2a-n**) (3.5 mmol) was added to a solution of 5-fluoro-1-methyl/ ethyl-1*H*-indole-2,3-diones **4**/ **5** (3.5 mmol) in ethanol (20 mL) or containing a catalytic amount of H_2SO_4 in ethanol (20 mL) (for **6a**, **6b**, **6d**, **6e**, **6l**, **7a** and **7b**). After the mixture was refluxed on a water bath. Completion of the reaction was controlled with TLC method. The product formed after cooling was filtered and washed with ethanol and recrystallized from ethanol.

4.1.5. 5-Fluoro-1-methyl-1H-indole-2,3-dione 3-[4-(phenyl) thiosemicarbazone] (6a)

Red powder (88%): mp 242–247 °C; IR (KBr): υ 3300, 3232 (NH), 1691 (C=O), 1276 (C=S). ^{1}H NMR (DMSO-d_6/ 500 MHz) ppm: 3.22 (3H, s, indole N-CH_3), 7.16 (1H, dd, J: 8.8, 3.9 Hz, indole C_7-H), 7.27–7.32 (2H, m, indole C_6-H, phenyl C_4-H), 7.43 (2H, t, J: 7.8 Hz, phenyl $C_{3,5}$-H), 7.60 (2H, d, J: 7.8 Hz, phenyl $C_{2,6}$-H), 7.67 (1H, dd, J: 8.0, 2.7 Hz, indole C_4-H), 10.76 (1H, s, N_4-H), 12.55 (1H, s, N_2-H). ^{13}C NMR (DECOUPLED DMSO-d_6/ 125 MHz): 26.46 (indole N-CH_3), 108.72 (d, J: 26.1 Hz, indole C_4), 111,59 (d, J: 8,4 Hz, indole C_7), 117.90 (d, J: 24.0 Hz, indole C_6), 121.24 (d, J: 9.6 Hz, indole C_{3a}), 126.20 (phenyl $C_{2,6}$), 126.82 (phenyl C_4), 129.02 (phenyl $C_{3,5}$), 131,28 (d, J: 2.7 Hz, indole C_3), 138.82 (phenyl C_1); 140.53 (indole C_{7a}), 159.24 (d, J: 237.9 Hz, indole C_5), 161.38 (indole C_2), 176.84 (C=S). LC/MS (ESI) $[M+H]^+$ $C_{16}H_{14}FN_4OS$: 329.37141; Found ($[M+H]^+$: 329.4. Anal. Calcd for $C_{16}H_{13}FN_4OS$: C, 58.52; H, 3.99; N, 17.06 Found: C, 58.46; H, 4.05; N, 16.72.

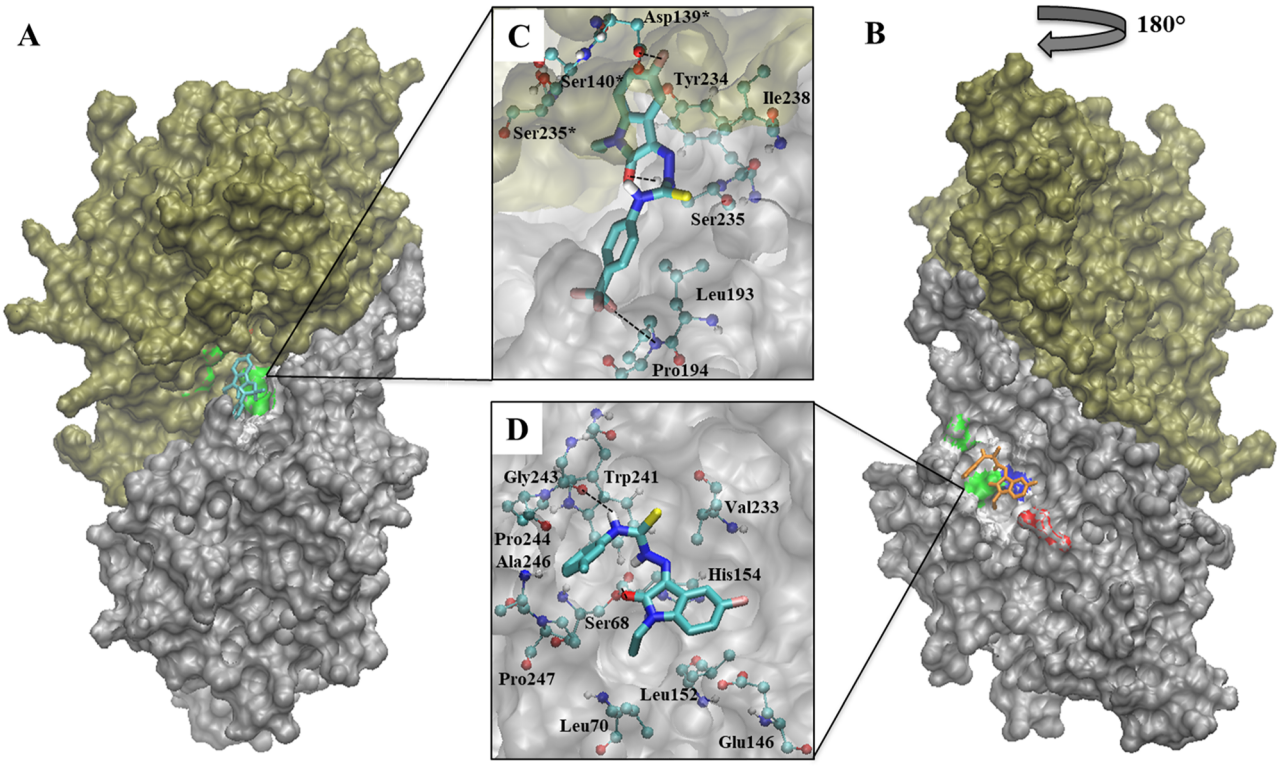

Fig. 4. A) Docking pose for compound **7d** in cyan, **B)** Docking pose for compound **7l** in orange on HSV-1 (gD) protein. In figure B orientation of protein was rotated 180°. Monomers are presented with gold and silver colors. Polar residues were shown in green, basic residues in blue, acidic residues in red, and hydrophobic residues in white. **C)** Zoomed in view of ligand **7d**. **D)** Zoomed in view of ligand **7l**. (For interpretation of the references to colour in this figure legend, the reader is referred to the web version of this article.)

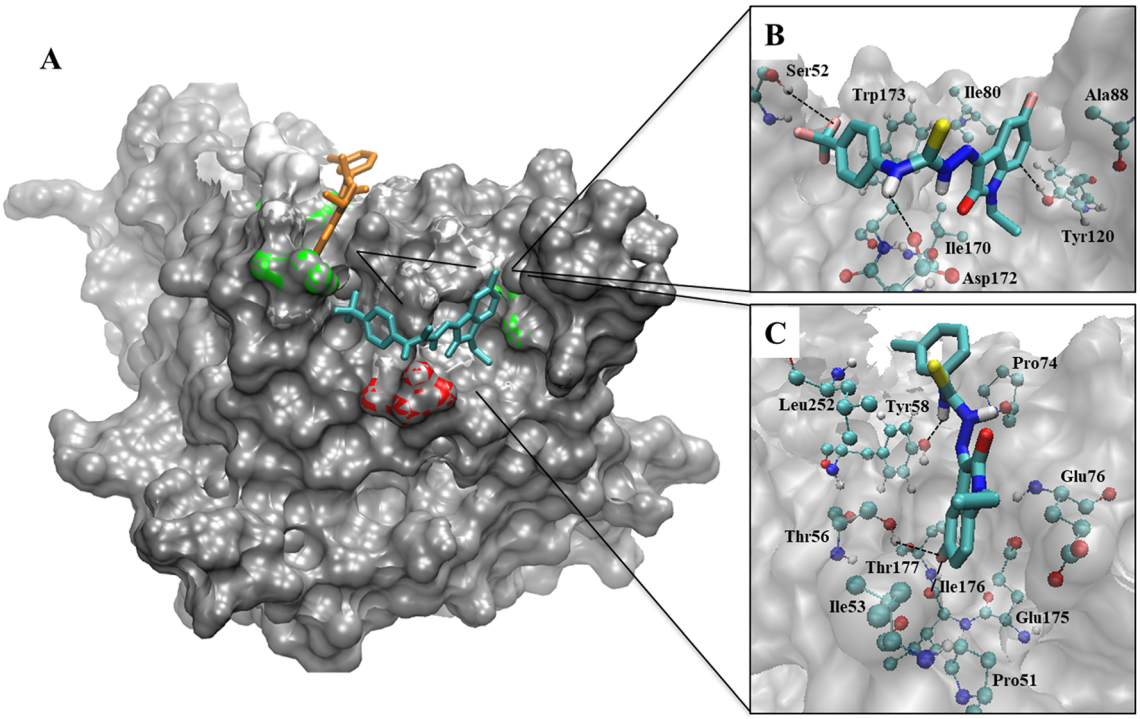

Fig. 5. A) Docking poses for compound **7d** in cyan, **7l** in orange, on HSV-2 (gD) protein. Polar residues were shown in green, acidic residues in red, and hydrophobic residues in white. **B)** Zoomed in view of ligand **7d**. **C)** Zoomed in view of ligand **7l**. (For interpretation of the references to colour in this figure legend, the reader is referred to the web version of this article.)

Table 5
Binding pockets on HSV-1 (gD) protein.

Compound	Interacting Amino Acids	Interaction Types	Binding Affinity (kcal/mol)
7d	Asp 139*	H-Bond	**−7.3**
	Ser 140*	Hydrophobic	
	Leu 193	Hydrophobic	
	Pro 194	H-Bond	
	Tyr 234	Hydrophobic	
	Ser 235	H-Bond	
	Ser 235*	Hydrophobic	
	Ile 238	Hydrophobic	
7l	Ser 68	H-Bond	**−7.2**
	Leu 70	Hydrophobic	
	Glu 146	Hydrophobic	
	Leu 152	Hydrophobic	
	His 154	Hydrophobic	
	Val 233	Hydrophobic	
	Trp 241	Hydrophobic	
	Gly 243	H-Bond	
	Pro 244	Hydrophobic	
	Ala 246	Hydrophobic	
	Pro 247	Hydrophobic	

* Amino acid residues of monomer 2 were shown by stars.

Table 6
Binding pockets on HSV-2 (gD) protein.

Compound	Interacting Amino Acids	Interaction Types	Binding Affinity (kcal/mol)
7d	Ser 52	H-Bond	**−7.4**
	Ile 80	Hydrophobic	
	Ala 88	Hydrophobic	
	Tyr 120	H-Bond	
	Ile 170	Hydrophobic	
	Asp 172	H-Bond	
	Trp 173	π-Stacking	
7l	Pro 51	Hydrophobic	**−7.5**
	Ile 53	Hydrophobic	
	Thr 56	H-Bond	
	Tyr 58	H-Bond	
	Pro 74	Hydrophobic	
	Glu 76	Hydrophobic	
	Glu 175	π-anion	
	Ile 176	Halogen Bond	
	Thr 177	H-Bond	
	Leu 252	Hydrophobic	

4.1.6. 5-Fluoro-1-methyl-1H-indole-2,3-dione 3-[4-(3-methylphenyl) thiosemicarbazone] (6b)

Orange powder (97%): mp 208–211 °C; IR (KBr): υ 3307, 3211 (NH), 1681 (C=O), 1278 (C=S). ^{1}H NMR (DMSO-d_6/ 400 MHz) ppm: 2.33 (3H, s, CH_3), 3.21 (3H, s, indole N-CH_3), 7.09 (1H, d, J: 7.6 Hz, phenyl C_4-H), 7.15 (1H, dd, J: 8.8, 4.0 Hz, indole C_7-H), 7.26–7.32 (2H, m, indole C_6-H, phenyl C_5-H), 7.39 (1H, s, phenyl C_2-H), 7.42 (1H, d, J: 8.0 Hz, phenyl C_6-H), 7.67 (1H, dd, J: 8.0, 2.4 Hz, indole C_4-H), 10.78 (1H, s, N_4-H), 12.56 (1H, s, N_2-H). ^{13}C NMR (DECOUPLED DMSO-d_6/ 100 MHz): 21.37 (CH_3), 26.31 (indole N-CH_3), 108.62 (d, J: 26.2 Hz, indole C_4), 111.42 (d, J: 8.3 Hz, indole C_7), 117.76 (d, J: 24.2 Hz, indole C_6), 121.10 (d, J: 9.6 Hz, indole C_{3a}), 123.09 (phenyl C_6), 126.40 (phenyl C_2), 127.32 (phenyl C_4), 128.71 (phenyl C_5), 131.05 (d, J: 3.2 Hz, indole C_3), 138.27 (phenyl C_1), 138.56 (phenyl C_3), 140.35 (indole C_{7a}), 159.12 (d, J: 238.1 Hz, indole C_5), 161.23 (indole C_2), 176.54 (C=S). HRMS (ESI) $[M+H]^+$ $C_{17}H_{16}FN_4OS$: 343.10234; Found $[M+H]^+$: 343.10223. Anal. Calcd for $C_{17}H_{15}FN_4OS$: C, 59.63; H, 4.42; N, 16.36 Found: C, 60.02; H, 4.48; N, 16.28.

4.1.7. 5-Fluoro-1-methyl-1H-indole-2,3-dione 3-[4-(4-methylphenyl) thiosemicarbazone] (6c)

Orange powder (88%): mp 224–227 °C; IR (KBr): υ 3319, 3232 (NH), 1683 (C=O), 1276 (C=S). ^{1}H NMR (DMSO-d_6/ 400 MHz) ppm: 2.31 (3H, s, CH_3), 3.21 (3H, s, indole N-CH_3), 7.15 (1H, dd, J: 8.6, 4.0 Hz, indole C_7-H); 7.21–7.23 (2H, m, AA′BB′ system, phenyl $C_{3,5}$-H), 7.28 (1H, td, J: 9.0, 2.8 Hz, indole C_6-H), 7.44–4.47 (2H, m, AA′BB′ system, phenyl $C_{2,6}$-H), 7.66 (1H, dd, J = 8.0, 2.8 Hz, indole C_4-H), 10.78 (1H, s, N_4-H, D_2O exch.), 12.55 (1H, s, N_2-H, D_2O exch). ^{13}C NMR (DECOUPLED DMSO-d_6/ 100 MHz): 21.08 (CH_3), 26.34 (indole N-CH_3), 108.60 (d, J: 26.2 Hz, indole C_4), 111.49 (d, J: 8.2 Hz, indole C_7), 117.76 (d, J: 24.1 Hz, indole C_6), 121.17 (d, J: 9.6 Hz, indole C_{3a}), 125.96 (phenyl $C_{2,6}$), 129.36 (phenyl $C_{3,5}$), 131.08 (d, J: 3.4 Hz, indole C_3), 136.00 (phenyl C_1), 136.14 (phenyl C_4), 140.40 (indole C_{7a}), 159.12 (d, J: 238.1 Hz, indole C_5), 161.29 (indole C_2), 176.70 (C=S). HRMS (ESI) $[M+H]^+$ $C_{17}H_{16}FN_4OS$: 343.10234; Found $[M+H]^+$: 343.10239. Anal. Calcd for $C_{17}H_{15}FN_4OS$: C, 59.63; H, 4.42; N, 16.36 Found: C, 59.75; H, 4.34; N, 16.25.

4.1.8. 5-Fluoro-1-methyl-1H-indole-2,3-dione 3-[4-(4-trifluoromethylphenyl)thiosemicarbazone] (6d)

Orange powder (86%): mp 217–220 °C; IR (KBr): υ 3278, 3224 (NH), 1681 (C=O), 1278 (C=S). ^{1}H NMR (DMSO-d_6/ 400 MHz) ppm: 3.21 (3H, s, indole N-CH_3), 7.16 (1H, dd, J: 8.8, 4.4 Hz, indole C_7-H), 7.30 (1H, td, J: 9.2, 2.8 Hz, indole C_6-H), 7.65 (1H, dd, J: 8.4, 2.8 Hz, indole C_4-H), 7.78–7.80 (2H, m, AA′BB′ system, phenyl $C_{2,6}$-H), 7.92–7.94 (2H, m, AA′BB′ system, phenyl $C_{3,5}$-H), 10.98 (1H, s, N_4-H), 12.71 (1H, s, N_2-H). ^{13}C NMR (DECOUPLED DMSO-d_6/ 100 MHz): 26.33 (indole N-CH_3), 108.69 (d, J: 26.1 Hz, indole C_4), 111.53 (d, J: 8.3 Hz, indole C_7), 118.01 (d, J: 24.1 Hz, indole C_6), 120.93 (d, J: 9.5 Hz, indole C_{3a}), 120.55, 123.25, 125.88, 125.91, 125.95, 125.98, 126.02, 126.35, 126.67, 126.99, 128.66, 142.41 (phenyl $C_{1,2,3,4,5,6}$, CF_3) 131.72 (d, J: 3.3 Hz, indole C_3), 140.53 (indole C_{7a}), 159.13 (d, J: 238.3 Hz, indole C_5), 161.25 (indole C_2), 176.68 (C=S). HRMS (ESI) $[M+H]^+$ $C_{17}H_{13}F_4N_4OS$: 397.07407; Found $[M+H]^+$: 397.07419. Anal. Calcd for $C_{17}H_{12}F_4N_4OS$: C, 51.51; H, 3.05; N, 14.14 Found: C, 50.94; H, 3.14; N, 14.15.

4.1.9. 5-Fluoro-1-methyl-1H-indole-2,3-dione 3-[4-(4-ethylphenyl)thiosemicarbazone] (6e)

Orange powder (94%): mp 193–196 °C; IR (KBr): υ 3290, 3207 (NH), 1681 (C=O), 1271 (C=S). ^{1}H NMR (DMSO-d_6/ 400 MHz) ppm: 1.19 (3H, t, J: 7.6 Hz, CH_2CH_3), 2.62 (2H, q, J: 7.6 Hz, CH_2CH_3), 3.21 (3H, s, indole N-CH_3), 7,15 (1H, dd, J: 8.6, 4.1 Hz, indole C_7-H), 7.24–7.31 (3H, m, AA′BB′ system phenyl $C_{3,5}$-H, indole C_6-H), 7.48–7.50 (2H, m, AA′BB′ system, phenyl $C_{2,6}$-H), 7.66 (1H, dd, J: 8.1, 2.7 Hz, indole C_4-H), 10.76 (1H, s, N_4-H); 12.56 (1H, s, N_2-H). ^{13}C NMR (HSQC-2D DMSO-d_6/ 125 MHz): 16.07 (CH_3), 26.38 (indole N-CH_3), 28.22 (CH_2), 108.61 (d, J: 26.6 Hz, indole C_4), 111.53 (indole C_7), 117.86 (indole C_6), 121.20 (d, J: 9.5 Hz, indole C_{3a}), 126.02 (phenyl $C_{2,6}$), 128.18 (phenyl $C_{3,5}$), 131.14 (indole C_3), 136.36 (phenyl C_1), 140.45 (indole C_{7a}), 142.35 (phenyl C_4), 159.16 (d, J: 237.7 Hz, indole C_5), 161.34 (indole C_2), 176.70 (C=S). Anal. Calcd for $C_{18}H_{17}FN_4OS$: C, 60.66; H, 4.81; N, 15.72 Found: C, 60.90; H, 5.09; N, 15.70.

4.1.10. 5-Fluoro-1-methyl-1H-indole-2,3-dione 3-[4-(3-methoxyphenyl) thiosemicarbazone] (6f)

Red powder (74%): mp 202–205 °C; IR (KBr): υ 3302, 3217 (NH), 1687 (C=O), 1259 (C=S). ^{1}H NMR (DMSO-d_6/ 400 MHz) ppm: 3.21 (3H, s, indole N-CH_3), 3.77 (3H, s, OCH_3), 6.85 (1H, dd, J: 8.2, 2.4 Hz, phenyl C_4-H), 7.14 (1H, dd, J: 8.6, 4.0 Hz. indole C_7-H), 7.22 (1H, d, J: 7.8 Hz, phenyl C_6-H), 7.26–7.34 (3H, m, indole C_6-H, phenyl $C_{2,5}$-H), 7.67 (1H, dd, J: 8.0, 2.6 Hz, indole C_4-H), 10.78 (1H, s, N_4-H), 12.58 (1H, s, N_2-H). ^{13}C NMR (DECOUPLED DMSO-d_6/ 100 MHz): 26.29 (indole N-CH_3), 55.69 (OCH_3), 108.66 (d, J: 26.2 Hz, indole C_4), 111.39 (d, J: 8.2 Hz, indole C_7), 111.51 (phenyl C_2), 112.10 (phenyl C_4), 117.76 (d, J: 24.2 Hz, indole C_6), 117.92 (phenyl C_6), 121.04 (d, J: 9.6 Hz, indole C_{3a}), 129.62 (phenyl C_5), 131.06 (d, J: 3.3 Hz, indole C_3), 139.77 (phenyl C_1), 140.33 (indole C_{7a}), 159.12 (d, J: 238.2 Hz, indole

C_5), 159.65 (phenyl C_3), 161.19 (indole C_2), 176.36 (C=S). HRMS (ESI) $[M+H]^+$ $C_{17}H_{16}FN_4O_2S$: 359.09725; Found $[M+H]^+$: 359.09711. Anal. Calcd for $C_{17}H_{15}FN_4O_2S$: C, 56.97; H, 4.22; N, 15.63 Found: C, 56.53; H, 4.26; N, 15.77.

4.1.11. 5-Fluoro-1-methyl-1H-indole-2,3-dione 3-[4-(4-methoxyphenyl) thiosemicarbazone] (6 g)

Orange powder (73%): mp 248–250 °C; IR (KBr): υ 3286, 3217 (NH), 1687 (C=O), 1257 (C=S). ^{1}H NMR (DMSO-d_6/ 500 MHz) ppm: 3.22 (3H, s, indole N-CH_3), 3.78 (3H, s, OCH_3), 6.97–7.00 (2H, m, AA′BB′ system, phenyl $C_{3,5}$-H), 7.16 (1H, dd, J: 8.5, 4.1 Hz, indole C_7-H), 7.30 (1H, td, J: 9.3, 2.9 Hz, indole C_6-H), 7.45–7.47 (2H, m, AA′BB′ system, phenyl $C_{2,6}$-H), 7.66 (1H, dd, J: 7.8, 2.4 Hz, indole C_4-H), 10.76 (1H, s, N_4-H), 12.55 (1H, s, N_2-H). ^{13}C NMR (DECOUPLED DMSO-d_6/ 100 MHz): 26.29 (indole N-CH_3), 55.75 (OCH_3), 108.53 (d, J: 26.2 Hz, indole C_4), 111.38 (d, J: 8.2 Hz, indole C_7), 114.08 (phenyl $C_{3,5}$), 117.66 (d, J: 24.2 Hz, indole C_6), 121.15 (d, J: 9.5 Hz, indole C_{3a}), 127.58 (phenyl $C_{2,6}$), 130.85 (d, J: 3.2 Hz, indole C_3), 131.53 (phenyl C_1), 140.29 (indole C_{7a}), 157.92 (phenyl C_4), 159.13 (d, J: 238.2 Hz, indole C_5), 161.21 (indole C_2), 176.87 (C=S). HRMS (ESI) $[M+H]^+$ $C_{17}H_{16}FN_4O_2S$: 359.09725; Found $[M+H]^+$: 359.09711. Anal. Calcd for $C_{17}H_{15}FN_4O_2S$: C, 56.97; H, 4.22; N, 15.63 Found: C, 57.08; H, 4.25; N, 15.70.

4.1.12. 5-Fluoro-1-methyl-1H-indole-2,3-dione 3-[4-(4-methylthiophenyl) thiosemicarbazone] (6h)

Red crystal (94%): mp 235–238 °C; IR (KBr): υ 3269, 3226 (NH), 1681 (C=O), 1274 (C=S). ^{1}H NMR (DMSO-d_6/ 400 MHz) ppm: 2.49 (3H, s, SCH_3), 3.21 (3H, s, indole N-CH_3), 7.15 (1H, dd, J: 8.6, 4.1 Hz, indole C_7-H), 7.26–7.31 (3H, m, indole C_6-H, AA′BB′ system phenyl $C_{3,5}$-H), 7.54–7.56 (2H, m, AA′BB′ system, phenyl $C_{2,6}$-H), 7.64 (1H, dd, J: 8.1, 2.7 Hz, indole C_4-H), 10.81 (1H, s, N_4-H), 12.57 (1H, s, N_2-H). ^{13}C NMR (HMBC-2D DMSO-d_6/ 125 MHz): 15.36 (SCH_3), 26.36 (indole N-CH_3), 108.62 (d, J: 25.7 Hz, indole C_4), 111.51 (d, J: 8.6 Hz, indole C_7), 117.82 (d, J: 23.7 Hz, indole C_6), 121.14 (d, J: 9.5 Hz, indole C_{3a}), 126.34 (phenyl $C_{2,6}$), 126.57 (phenyl $C_{3,5}$), 131.18 (d, J: 3.9 Hz, indole C_3), 135.77 (phenyl C_1), 136.34 (phenyl C_4), 140.44 (indole C_{7a}), 159.16 (d, J: 237.7 Hz, indole C_5), 161.29 (indole C_2), 176.62 (C=S). Anal. Calcd for $C_{17}H_{15}FN_4OS_2$: C, 54.53; H, 4.04; N, 14.96 Found: C, 54.24; H, 4.09; N, 14.99.

4.1.13. 5-Fluoro-1-methyl-1H-indole-2,3-dione 3-[4-(4-trifluoromethoxyphenyl)thiosemicarbazone] (6i)

Orange powder (81%): mp 214–217 °C; IR (KBr): υ 3317, 3224 (NH), 1674 (C=O), 1276 (C=S). ^{1}H NMR (DMSO-d_6/ 400 MHz) ppm: 3.21 (3H, s, indole N-CH_3), 7.16 (1H, dd, J: 8.6, 4.4 Hz, indole C_7-H), 7.29 (1H, td, J: 9.2, 2.8 Hz, indole C_6-H), 7.41–7.43 (2H, m, AA′BB′ system, phenyl $C_{3,5}$-H), 7.63 (1H, dd, J: 8.4, 2.8 Hz, indole C_4-H), 7.72–7.76 (2H, m, AA′BB′ system, phenyl $C_{2,6}$-H), 10.89 (1H, s, N_4-H), 12.64 (1H, s, N_2-H). ^{13}C NMR (DECOUPLED DMSO-d_6/ 100 MHz): 26.35 (indole N-CH_3), 108.60 (d, J: 26.1 Hz, indole C_4), 111.57 (d, J: 8.3 Hz, indole C_7), 117.96 (d, J: 24.2 Hz, indole C_6), 120.53 (d, J: 256.2 Hz, OCF_3), 121.04 (d, J: 9.5 Hz, indole C_{3a}), 121.57 (phenyl $C_{2,6}$), 127.83 (phenyl $C_{3,5}$), 131.58 (d, J: 3.3 Hz, indole C_3), 137.87 (phenyl C_4), 140.55 (indole C_{7a}), 146.38 (q, J: 1.7 Hz, phenyl C_1), 159.12 (d, J: 238.2 Hz, indole C_5), 161.30 (indole C_2), 176.98 (C=S). HRMS (ESI) $[M+H]^+$ $C_{17}H_{13}F_4N_4O_2S$: 413.06899; Found $[M+H]^+$: 413.06900. Anal. Calcd for $C_{17}H_{12}F_4N_4O_2S$: C, 49.52; H, 2.93; N, 13.59 Found: C, 49.58; H, 2.89; N, 13.67.

4.1.14. 5-Fluoro-1-methyl-1H-indole-2,3-dione 3-[4-(3-fluorophenyl) thiosemicarbazone] (6j)

Orange crystal (82%): mp 237–243 °C; IR (KBr): υ 3288, 3226 (NH), 1695 (C=O), 1276 (C=S). ^{1}H NMR (DMSO-d_6/ 400 MHz) ppm: 3.20 (3H, s, indole N-CH_3), 7.09–7.16 (1H, m, phenyl C_4-H), 7.14 (1H, dd, J: 8.7, 3.9 Hz, indole C_7-H), 7.28 (1H, td, J: 9.0, 2.7 Hz, indole C_6-H), 7.43–7.51 (2H, m, phenyl $C_{5,6}$-H), 7.59–7.65 (2H, m, indole C_4-H, phenyl C_2-H), 10.86 (1H, s, N_4-H), 12.62 (1H, s, N_2-H). ^{13}C NMR (DECOUPLED DMSO-d_6/ 125 MHz): 26.48 (indole N-CH_3), 108.79 (d, J: 26.2 Hz, indole C_4), 111.67 (d, J: 8.4 Hz, indole C_7), 112.80 (d, J: 24.9 Hz, phenyl C_2), 113.40 (d, J: 26.0 Hz, phenyl C_4), 118.08 (d, J: 21.8 Hz, indole C_6), 121.14 (d, J: 9.5 Hz, indole C_{3a}), 121.81 (phenyl C_6), 130.57 (d, J: 9.5 Hz, phenyl C_5), 131.67 (d, J: 3.2 Hz, indole C_3), 140.50 (d, J: 10.8 Hz, phenyl C_1), 140.66 (indole C_{7a}), 159.25 (d, J: 238.3 Hz, indole C_5), 161.40 (indole C_2), 162.18 (d, J: 242.7 Hz, phenyl C_3), 176.71 (C=S). Anal. Calcd for $C_{16}H_{12}F_2N_4OS$: C, 55.48; H, 3.49; N, 16.18 Found: C, 55.26; H, 3.41; N, 16.18.

4.1.15. 5-Fluoro-1-methyl-1H-indole-2,3-dione 3-[4-(4-fluorophenyl) thiosemicarbazone] (6k)

Orange powder (76%): mp 258–262 °C; IR (KBr): υ 3327, 3302, 3201 (NH), 1681 (C=O), 1271 (C=S). ^{1}H NMR (DMSO-d_6/ 400 MHz) ppm: 3.21 (3H, s, indole N-CH_3), 7.15 (1H, dd, J: 8.6, 4.2 Hz, indole C_7-H), 7.23–7.31 (3H, m, AA′BB′ system phenyl $C_{3,5}$-H, indole C_6-H), 7.58–7.61 (2H, m, AA′BB′ system, phenyl $C_{2,6}$-H), 7.64 (1H, dd, J: 8.0, 2.8 Hz, indole C_4-H), 10.82 (1H, s, N_4-H), 12.59 (1H, s, N_2-H). ^{13}C NMR (DECOUPLED DMSO-d_6/ 125 MHz): 26.45 (indole N-CH_3), 108.65 (d, J: 26.6 Hz, indole C_4), 111.61 (d, J: 8.1 Hz, indole C_7), 115.76 (d, J: 20.0 Hz, phenyl $C_{3,5}$), 117.94 (d, J: 23.9 Hz, indole C_6), 121.20 (d, J: 9.5 Hz, indole C_{3a}), 128.48 (d, J: 8.4 Hz, phenyl $C_{2,6}$), 131.39 (d, J: 3.1 Hz, indole C_3), 135.16 (d, J: 2.6 Hz, phenyl C_1), 140.56 (indole C_{7a}), 159.22 (d. J: 238.6 Hz. indole C_5), 160.63 (d. J: 243.2 Hz. phenyl C_4), 161.37 (indole C_2), 177.23 (C=S). LC/MS ESI $[M+H]^+$ $C_{16}H_{13}F_2N_4OS$: 347.36187; Found $[M+H]^+$: 347.4. Anal. Calcd for $C_{16}H_{12}F_2N_4OS$: C, 55.48; H, 3.49; N, 16.18 Found: C, 55.52; H, 3.57; N, 16.16.

4.1.16. 5-Fluoro-1-methyl-1H-indole-2,3-dione 3-[4-(3-chlorophenyl) thiosemicarbazone] (6l)

Orange powder (94%): mp 238–240 °C; IR (KBr): υ 3336, 3219 (NH), 1695 (C=O), 1273 (C=S). ^{1}H NMR (DMSO-d_6/ 400 MHz) ppm: 3.21 (3H, s, indole N-CH_3), 7.16 (1H, dd, J: 8.6, 4.0 Hz, indole C_7-H), 7.28–7.35 (2H, m, indole C_6-H, phenyl C_4-H), 7.45 (1H, t, J: 8.0 Hz, phenyl C_5-H), 7.63–7.66 (2H, m, phenyl C_6-H, indole C_4-H), 7.77 (1H, t, J: 2.0 Hz, phenyl C_2-H), 10.88 (1H, s, N_4-H), 12.64 (1H, s, N_2-H). ^{13}C NMR (DECOUPLED DMSO-d_6/ 100 MHz): 26.35 (indole N-CH_3), 108.66 (d, J: 26.4 Hz, indole C_4), 111.54 (d, J: 8.6 Hz, indole C_7), 117.97 (d, J: 24.0 Hz, indole C_6), 120.99 (d, J: 9.7 Hz, indole C_{3a}), 124.39 (phenyl C_6), 125.42 (phenyl C_2), 126.40 (phenyl C_4), 130.48 (phenyl C_5), 131.57 (d, J: 3.2 Hz, indole C_3), 132.97 (phenyl C_3), 140.16 (phenyl C_1), 140.53 (indole C_{7a}), 159.13 (d, J: 238.2 Hz, indole C_5), 161.27 (indole C_2), 176.65 (C=S). HRMS (ESI) $[M+H]^+$ $C_{16}H_{13}ClFN_4OS$: 363.04771; 365.04476 Found $[M+H]^+$: 363.04761; 365.04465. Anal. Calcd for $C_{16}H_{12}ClFN_4OS$: C, 52.97; H, 3.33; N, 15.44 Found: C, 53.16; H, 3.40; N, 15.53.

4.1.17. 5-Fluoro-1-methyl-1H-indole-2,3-dione 3-[4-(4-chlorophenyl) thiosemicarbazone] (6m)

Red powder (85%): mp 269–273 °C; IR (KBr): υ 3315, 3230 (NH), 1681 (C=O), 1278 (C=S). ^{1}H NMR (DMSO-d_6/ 400 MHz) ppm: 3.21 (3H, s, indole N-CH_3), 7.15 (1H, dd, J: 8.6, 4.1 Hz, indole C_7-H), 7.29 (1H, td, J: 9.4, 2.7 Hz, indole C_6-H), 7.46–7.50 (2H, m, AA′BB′ system, phenyl $C_{3,5}$-H), 7.62–7.67 (3H, m, indole C_4-H, AA′BB′ system phenyl $C_{2,6}$-H), 10.85 (1H, s, N_4-H), 12.63 (1H, s, N_2-H). ^{13}C NMR (HSQC-2D DMSO-d_6/ 125 MHz): 26.36 (indole N-CH_3), 108.69 (d, J: 30.5 Hz, indole C_4), 111.58 (indole C_7), 118.13 (indole C_6), 121.03 (d, J: 9.5 Hz, indole C_{3a}), 127.81 (phenyl $C_{2,6}$), 128.90 (phenyl $C_{3,5}$), 130.79 (phenyl C_4), 131.63 (d, J: 2.9 Hz, indole C_3), 137.68 (phenyl C_1), 140.54 (indole C_{7a}), 159.15 (d, J: 238.7 Hz, indole C_5), 161.34 (indole C_2), 176.89 (C=S). LC/MS ESI $[M+H]^+$ $C_{16}H_{13}ClFN_4OS$: 363.81647; Found $[M+H]^+$: 363.3; 365.6. Anal. Calcd for $C_{16}H_{12}ClFN_4OS$: C, 52.97; H, 3.33; N, 15.44 Found: C, 52.96; H, 3.34; N, 15.42.

4.1.18. 5-Fluoro-1-methyl-1H-indole-2,3-dione 3-[4-(4-bromophenyl) thiosemicarbazone] (6n)

Red powder (86%): mp 248–251 °C; IR (KBr): υ 3309, 3296, 3230 (NH), 1681 (C=O), 1278 (C=S). ^{1}H NMR (DMSO-d_6/ 500 MHz) ppm: 3.22 (3H, s, indole N-CH_3), 7.16 (1H, dd, *J:* 8.5, 4.1 Hz, indole C_7-H), 7.30 (1H, td, *J:* 9.3, 2.9 Hz, indole C_6-H), 7.59–7.62 (4H, m, AA′BB′ system, phenyl $C_{2,3,5,6}$-H), 7.65 (1H, dd, *J:* 8.0, 2.7 Hz, indole C_4-H), 10.85 (1H, s, N_4-H), 12.64 (1H, s, N_2-H). ^{13}C NMR (DECOUPLED DMSO-d_6/ 125 MHz): 26.48 (indole N-CH_3), 108.72 (d, *J:* 26.2 Hz, indole C_4), 111.65 (d, *J:* 7,2 Hz, indole C_7), 118.03 (d, *J:* 22.0 Hz, indole C_6), 119.11 (phenyl C_4), 121.16 (d, *J:* 9.5 Hz, indole C_{3a}), 128.10 (phenyl $C_{2,6}$), 131.60 (d, *J:* 3.3 Hz, indole C_3), 131.89 (phenyl $C_{3,5}$), 138.24 (phenyl C_1), 140.64 (indole C_{7a}), 159.23 (d, *J:* 238.2 Hz, indole C_5), 161.40 (indole C_2), 176.82 (C=S). LC/MS ESI $[M+H]^+$ $C_{16}H_{13}BrFN_4OS$: 408.26747; Found $[M+H]^+$: 407.2; 409.3. Anal. Calcd for $C_{16}H_{12}BrFN_4OS$: C, 47.19; H, 2.97; N, 13.76 Found: C, 47.22; H, 3.11; N, 13.64.

4.1.19. 1-Ethyl-5-fluoro-1H-indole-2,3-dione 3-[4-(phenyl)thiosemicarbazone] (7a)

Yellow powder (99%): mp 203–205 °C; IR (KBr): υ 3292, 3209 (NH), 1683 (C=O), 1271 (C=S). ^{1}H NMR (DMSO-d_6/ 500 MHz) ppm: 1.20 (3H, t, J: 7.3 Hz, indole N-CH_2CH_3), 3.79 (2H, q, J: 7.3 Hz, indole N-CH_2CH_3), 7.22 (1H, dd, J: 8.5, 4.1 Hz, indole C_7-H), 7.26–7.30 (2H, m, indole C_6-H, phenyl C_4-H), 7.43 (2H, t, J: 7.8 Hz, phenyl $C_{3,5}$-H), 7.61 (2H, d, J: 8.3 Hz, phenyl $C_{2,6}$-H), 7.69 (1H, dd, J: 8.1, 2.7 Hz, indole C_4-H), 10.84 (1H, s, N_4-H), 12.62 (1H, s, N_2-H). ^{13}C NMR (HSQC-2D DMSO-d_6/ 125 MHz): 13.03 (indole N-CH_2CH_3), 34.70 (indole N-CH_2CH_3), 108.82 (d, J: 26.7 Hz, indole C_4), 111.59 (indole C_7), 117.87 (d, J: 24.7 Hz, indole C_6), 121.37 (d, J: 9.5 Hz, indole C_{3a}), 126.09 (phenyl $C_{2,6}$), 126.73 (phenyl C_4), 128.95 (phenyl $C_{3,5}$), 131.24 (d, J: 3.9 Hz, indole C_3), 138.73 (phenyl C_1), 139.37 (indole C_{7a}), 159.08 (d, J: 237.8 Hz, indole C_5), 160.95 (indole C_2), 176.75 (C=S). Anal. Calcd for $C_{17}H_{15}FN_4OS$: C, 59.63; H, 4.42; N, 16.36 Found: C, 59.86; H, 4.66; N, 16.36.

4.1.20. 1-Ethyl-5-fluoro-1H-indole-2,3-dione 3-[4-(3-methylphenyl) thiosemicarbazone] (7b)

Orange powder (91%): mp 181–184 °C; IR (KBr): υ 3315, 3215 (NH), 1678 (C=O), 1273 (C=S). ^{1}H NMR (DMSO-d_6/ 400 MHz) ppm: 1.19 (3H, t, J: 7.2 Hz, indole N-CH_2CH_3), 2.33 (3H, s, CH_3), 3.78 (2H, q, J: 7.2 Hz, indole N-CH_2CH_3), 7.09 (1H, d, J: 7.5 Hz, phenyl C_4-H), 7.22 (1H, dd, J: 8.7, 4.2 Hz, indole C_7-H), 7.25–7.32 (2H, m, indole C_6-H, phenyl C_5-H), 7.40 (1H, s, phenyl C_2-H), 7.42 (1H, d, J: 7.7 Hz, phenyl C_6-H), 7.69 (1H, dd, J: 8.1, 2.6 Hz, indole C_4-H), 10.79 (1H, s, N_4-H), 12.58 (1H, s, N_2-H). ^{13}C NMR (HSQC-2D DMSO-d_6/ 125 MHz): 13.02 (indole N-CH_2CH_3), 21.38 (CH_3), 34.70 (indole N-CH_2CH_3), 108.84 (d, J: 26.6 Hz, indole C_4), 111.57 (indole C_7), 117.86 (d, J: 24.8 Hz, indole C_6), 121.37 (d, J: 9.5 Hz, indole C_{3a}), 123.10 (phenyl C_6), 126.43 (phenyl C_2), 127.31 (phenyl C_4), 128.74 (phenyl C_5), 131.17 (d, J: 3.9 Hz, indole C_3), 138.31 (phenyl C_1), 138.61 (phenyl C_3), 139.35 (indole C_{7a}), 159.08 (d, J: 238.8 Hz, indole C_5), 160.95 (indole C_2), 176.59 (C=S). LC/MS ESI $[M+H]^+$ $C_{18}H_{18}FN_4OS$: 357.42457; Found $[M+H]^+$: 357.5. Anal. Calcd for $C_{18}H_{17}FN_4OS$: C, 60.66; H, 4.81; N, 15.72 Found: C, 60.65; H, 4.47; N, 15.42.

4.1.21. 1-Ethyl-5-fluoro-1H-indole-2,3-dione 3-[4-(4-methylphenyl) thiosemicarbazone] (7c)

Orange powder (85%): mp 159–161 °C; IR (KBr): υ 3311, 3226 (NH), 1685 (C=O), 1273 (C=S). ^{1}H NMR (DMSO-d_6/ 400 MHz) ppm: 1.19 (3H, t, J: 7.2 Hz, indole N-CH_2CH_3), 2.31 (3H, s, CH_3), 3.78 (2H, q, J: 7.2 Hz, indole N-CH_2CH_3), 7.20–7.23 (3H, m, indole C_7-H, AA′BB′ system, phenyl $C_{3,5}$-H), 7.28 (1H, td, J: 9.0, 2.8 Hz, indole C_6-H), 7.45–7.47 (2H, m, AA′BB′ system, phenyl $C_{2,6}$-H), 7.67 (1H, dd, J: 8.0, 2.8 Hz, indole C_4-H), 10.78 (1H, s, N_4-H), 12.58 (1H, s, N_2-H). ^{13}C NMR (DECOUPLED DMSO-d_6/ 125 MHz): 13.04 (indole N-CH_2CH_3), 21.09 (CH_3), 34.68 (indole N-CH_2CH_3), 108.79 (d, J: 26.3 Hz, indole C_4), 111.56 (d, J: 8.4 Hz, indole C_7), 117.80 (d, J: 23.9 Hz, indole C_6), 121.39 (d, J: 9.5 Hz, indole C_{3a}), 125.93 (phenyl $C_{2,6}$), 129.38 (phenyl $C_{3,5}$), 131.09 (d, J: 3.2 Hz, indole C_3), 135.99 (phenyl C_1), 136.17 (phenyl C_4), 139.32 (indole C_{7a}), 159.06 (d, J: 238.2 Hz, indole C_5), 160.93 (indole C_2), 176.69 (C=S). LC/MS ESI $[M+H]^+$ $C_{18}H_{18}FN_4OS$: 357.42457; Found $[M+H]^+$: 357.5. Anal. Calcd for $C_{18}H_{17}FN_4OS$: C, 60.66; H, 4.81; N, 15.72 Found: C, 60.85; H, 4.82; N, 15.60.

4.1.22. 1-Ethyl-5-fluoro-1H-indole-2,3-dione 3-[4-(4-trifluoromethylphenyl)thiosemicarbazone] (7d)

Orange powder (78%): mp 199–202 °C; IR (KBr): υ 3282, 3211 (NH), 1695 (C=O), 1271 (C=S). ^{1}H NMR (DMSO-d_6/ 400 MHz) ppm: 1.19 (3H, t, J: 7.2 Hz, indole N-CH_2CH_3), 3.78 (2H, q, J: 7.2 Hz, indole N-CH_2CH_3), 7.23 (1H, dd, *J:* 8.7, 4.2 Hz, indole C_7-H), 7.30 (1H, td, *J:* 9.0, 2.7 Hz, indole C_6-H), 7.67 (1H, dd, *J:* 8.0, 2.6 Hz, indole C_4-H), 7.78–7.80 (2H, m, AA′BB′ system, phenyl $C_{2,6}$-H), 7.92–7.94 (2H, m, AA′BB′ system, phenyl $C_{3,5}$-H), 11,00 (1H. s, N_4-H), 12.73 (1H, s, N_2-H). ^{13}C NMR (DECOUPLED DMSO-d_6/ 100 MHz): 12.96 (indole N-CH_2CH_3), 34.69 (indole N-CH_2CH_3), 108.90 (d, J: 26.0 Hz, indole C_4), 111.59 (d, J: 8.1 Hz, indole C_7), 118.04 (d, J: 24.1 Hz, indole C_6), 121.13 (d, J: 9.5 Hz, indole C_{3a}), 120.54, 123.25, 125.83, 125.89, 125.93, 125.97, 126.01, 126.33, 126.65, 126.97, 128.65, 142.40 (phenyl $C_{1,2,3,4,5,6}$, CF_3), 131.76 (d, J: 3.3 Hzj indole C_3), 139.46 (indole C_{7a}), 159.04 (d, J: 238.4 Hz, indole C_5), 160.88 (indole C_2), 176.64 (C=S). HRMS (ESI) $[M+H]^+$ $C_{18}H_{15}F_4N_4OS$: 411.08972; Found $[M+H]^+$: 411.08969. Anal. Calcd for $C_{18}H_{14}F_4N_4OS$: C, 52.68; H, 3.44; N, 13.65 Found: C, 52.59; H, 3.58; N, 13.81.

4.1.23. 1-Ethyl-5-fluoro-1H-indole-2,3-dione 3-[4-(4-ethylphenyl)thiosemicarbazone] (7e)

Orange powder (99%): mp 124–127 °C; IR (KBr): υ 3348, 3197 (NH), 1695 (C=O), 1271 (C=S). ^{1}H NMR (DMSO-d_6/ 400 MHz) ppm: 1.18 (3H, t, *J:* 7.6 Hz, CH_2CH_3), 1.19 (3H, t, *J:* 7.2 Hz, indole N-CH_2CH_3), 2.62 (2H, q, J: 7.6 Hz, CH_2CH_3), 3.78 (2H, q, J: 7.2 Hz, indole N-CH_2CH_3), 7.21 (1H, dd, J: 8.6, 4.2 Hz, indole C_7-H), 7.24–7.30 (3H, m, AA′BB′ system phenyl $C_{3,5}$-H, indole C_6-H), 7.48–7.50 (2H, m, AA′BB′ system, phenyl $C_{2,6}$-H), 7.67 (1H, dd, J: 8.0, 2.6 Hz, indole C_4-H), 10.77 (1H, s, N_4-H), 12.58 (1H, s, N_2-H). ^{13}C NMR (DECOUPLED DMSO-d_6/ 100 MHz): 13.01 (indole N-CH_2CH_3), 16.04 (CH_3), 28.20 (CH_2), 34.66 (indole N-CH_2CH_3), 108.78 (d, J: 26.0 Hz, indole C_4), 111.49 (d, J: 8.1 Hz, indole C_7), 117.76 (d, J: 24.1 Hz, indole C_6), 121.33 (d, J: 9.5 Hz, indole C_{3a}), 125.93 (phenyl $C_{2,6}$), 128.13 (phenyl $C_{3,5}$), 131.02 (d, J: 3.3 Hz, indole C_3), 136.33 (phenyl C_1), 139.26 (indole C_{7a}), 142.27 (phenyl C_4), 159.04 (d, J: 238.1 Hz, indole C_5), 160.88 (indole C_2), 176.59 (C=S). HRMS (ESI) $[M+H]^+$ $C_{19}H_{20}FN_4OS$: 371.13364; Found $[M+H]^+$: 371.13361. Anal. Calcd for $C_{19}H_{19}FN_4OS$: C, 61.60; H, 5.17; N, 15.12 Found: C, 61.93; H, 5.15; N, 15.10.

4.1.24. 1-Ethyl-5-fluoro-1H-indole-2,3-dione 3-[4-(3-methoxyphenyl) thiosemicarbazone] (7f)

Orange powder (90%): mp 159–162 °C; IR (KBr): υ 3302, 3217 (NH), 1681 (C=O), 1276 (C=S). ^{1}H NMR (DMSO-d_6/ 400 MHz) ppm: 1.19 (3H, t, J: 7.2 Hz, indole N-CH_2CH_3), 3.77 (3H, s, OCH_3), 3.78 (2H, q, J: 7.2 Hz, indole N-CH_2CH_3), 6.85 (1H, ddd, J: 8.3, 2.5, 0.8 Hz, phenyl C_4-H), 7.20–7.34 (5H, m, indole $C_{6,7}$-H, phenyl $C_{2,5,6}$-H), 7.69 (1H, dd, J: 8.1, 2.6 Hz, indole C_4-H), 10.79 (1H, s, N_4-H), 12.61 (1H, s, N_2-H). ^{13}C NMR (HSQC-2D DMSO-d_6/ 125 MHz): 13.23 (indole N-CH_2CH_3), 34.90 (indole N-CH_2CH_3), 55.92 (OCH_3), 109.10 (d, J: 25.7 Hz, indole C_4), 111.51 (phenyl C_2), 111.74 (indole C_7), 112.33 (phenyl C_4), 117.68 (phenyl C_6), 118.14 (indole C_6), 121.54 (d, J: 9.5 Hz, indole C_{3a}), 129.86 (phenyl C_5), 131.44 (indole C_3), 139.58 (phenyl C_1), 140.02 (indole C_{7a}), 159.28 (d, J: 238.7 Hz, indole C_5), 159.90 (phenyl C_3), 161.15 (indole C_2), 176.63 (C=S). LC/MS ESI $[M+H]^+$ $C_{18}H_{17}FN_4O_2S$: 373.42397; Found $[M+H]^+$: 373.4. Anal. Calcd

for $C_{18}H_{17}FN_4O_2S$: C, 58.05; H, 4.60; N, 15.04 Found: C, 57.88; H, 4.79; N, 15.12.

4.1.25. 1-Ethyl-5-fluoro-1H-indole-2,3-dione 3-[4-(4-methoxyphenyl) thiosemicarbazone] (7g)

Orange powder (98%): mp 175–177 °C; IR (KBr): υ 3354, 3196 (NH), 1681 (C=O), 1253 (C=S). ^{1}H NMR (DMSO-d_6/ 400 MHz) ppm: 1.19 (3H, t, J: 7.2 Hz, indole N-CH_2CH_3), 3.77 (3H, s, OCH_3), 3.78 (2H, q, J: 7.2 Hz, indole N-CH_2CH_3), 6.96–6.98 (2H, m, AA′BB′ system, phenyl $C_{3,5}$-H), 7.21 (1H, dd, J: 8.8, 4.4 Hz, indole C_7-H), 7.27 (1H, td, J: 8.8, 2.4 Hz, indole C_6-H), 7.45–7.47 (2H, m, AA′BB′ system, phenyl $C_{2,6}$-H), 7.67 (1H, dd, J: 7.8, 2.4 Hz, indole C_4-H), 10.73 (1H, s, N_4-H), 12.56 (1H, s, N_2-H). ^{13}C NMR (DECOUPLED DMSO-d_6/ 100 MHz): 13.01 (indole N-CH_2CH_3), 34.66 (indole N-CH_2CH_3), 55.74 (OCH_3), 108.73 (d, J: 26.1 Hz, indole C_4), 111.49 (d, J: 8.2 Hz, indole C_7), 114.07 (phenyl $C_{3,5}$), 117.72 (d, J: 24.1 Hz, indole C_6), 121.37 (d, J: 9.5 Hz, indole C_{3a}), 127.56 (phenyl $C_{2,6}$), 130.93 (d, J: 3.2 Hz, indole C_3), 131.53 (phenyl C_1), 139.25 (indole C_{7a}), 157.91 (phenyl C_4), 159.04 (d, J: 238.2 Hz, indole C_5), 160.89 (indole C_2), 176.86 (C=S). HRMS (ESI) $[M+H]^+$ $C_{18}H_{18}FN_4O_2S$: 373.11290; Found $[M+H]^+$: 373.11279. Anal. Calcd for $C_{18}H_{17}FN_4O_2S$: C, 58.05; H, 4.60; N, 15.04 Found: C, 58.23; H, 4.76; N, 15.22.

4.1.26. 1-Ethyl-5-fluoro-1H-indole-2,3-dione 3-[4-(4-methylthiophenyl) thiosemicarbazone] (7h)

Orange powder (80%): mp 171–173 °C; IR (KBr): 3302, 3228 (NH), 1681 (C=O), 1273 (C=S). ^{1}H NMR (DMSO-d_6/ 400 MHz) ppm: 1.19 (3H, t, J: 7.2 Hz, indole N-CH_2CH_3), 2.49 (3H, s, SCH_3), 3.78 (2H, q, J: 7.2 Hz, indole N-CH_2CH_3), 7.22 (1H, dd, J: 8.6, 4.2 Hz, indole C_7-H), 7.26–7.31 (3H, m, indole C_6-H, AA′BB′ system phenyl $C_{3,5}$-H), 7.54–7.56 (2H, m, AA′BB′ system, phenyl $C_{2,6}$-H), 7.66 (1H, dd, J: 8.0, 2.6 Hz, indole C_4-H), 10.81 (1H, s, N_4-H), 12.61 (1H, s, N_2-H). ^{13}C NMR (DECOUPLED DMSO-d_6/ 100 MHz): 13.01 (indole N-CH_2CH_3), 15.37 (SCH_3), 34.68 (indole N-CH_2CH_3), 108.79 (d, J: 26.0 Hz, indole C_4), 111.52 (d, J: 8.1 Hz, indole C_7), 117.81 (d, J: 24.1 Hz, indole C_6), 121.30 (d, J: 9.5 Hz, indole C_{3a}), 126.31 (phenyl $C_{2,6}$), 126.47 (phenyl $C_{3,5}$), 131.17 (d, J: 3.3 Hz, indole C_3), 135.75 (phenyl C_1), 136.27 (phenyl C_4), 139.31 (indole C_{7a}), 159.04 (d, J: 238.2 Hz, indole C_5), 160.89 (indole C_2), 176.56 (C=S). HRMS (ESI) $[M+H]^+$ $C_{18}H_{18}FN_4OS_2$: 389.09006; Found $[M+H]^+$: 389.09003. Anal. Calcd for $C_{18}H_{17}FN_4OS_2$: C, 55.65; H, 4.41; N, 14.42 Found: C, 55.38; H, 4.52; N, 14.50.

4.1.27. 1-Ethyl-5-fluoro-1H-indole-2,3-dione 3-[4-(4-trifluoromethoxyphenyl)thiosemicarbazone] (7i)

Yellow powder (94%): mp 150–153 °C; IR (KBr): 3278, 3236 (NH), 1701 (C=O), 1267 (C=S). ^{1}H NMR (DMSO-d_6/ 400 MHz) ppm: 1.20 (3H, t, J: 7.2 Hz, indole N-CH_2CH_3), 3.78 (2H, q, J: 7.2 Hz, indole N-CH_2CH_3), 7.22 (1H, dd, J: 8.6, 4.2 Hz, indole C_7-H), 7.28 (1H, td, J: 9.0, 2.4 Hz, indole C_6-H), 7.41–7.43 (2H, m, AA′BB′ system, phenyl $C_{3,5}$-H), 7.64 (1H, dd, J: 8.0, 2.8 Hz, indole C_4-H), 7.72–7.76 (2H, m, AA′BB′ system, phenyl $C_{2,6}$-H), 10.89 (1H, s, N_4-H), 12.66 (1H, s, N_2-H). ^{13}C NMR (DECOUPLED DMSO-d_6/ 100 MHz): 12.97 (indole N-CH_2CH_3), 34.69 (indole N-CH_2CH_3), 108.79 (d, J: 26.1 Hz, indole C_4), 111.59 (d, J: 8.1 Hz, indole C_7), 117.95 (d, J: 24.1 Hz, indole C_6), 120.53 (q, J: 256.3 Hz, OCF_3), 121.22 (d, J: 9.5 Hz, indole C_{3a}), 121.54 (phenyl $C_{2,6}$), 127.75 (phenyl $C_{3,5}$), 131.54 (d, J: 3.3 Hz, indole C_3), 137.86 (phenyl C_4), 139.42 (indole C_{7a}), 146.36 (q, J: 1.8 Hz, phenyl C_1), 159.04 (d, J: 238.3 Hz, indole C_5), 160.90 (indole C_2), 176.92 (C=S). HRMS (ESI) [$[M+H]^+$ $C_{18}H_{15}F_4N_4O_2S$: 427.08464; Found $[M+H]^+$: 427.08472. Anal. Calcd for $C_{18}H_{14}F_4N_4O_2S$: C, 50.70; H, 3.31; N, 13.14 Found: C, 50.53; H, 3.36; N, 13.23.

4.1.28. 1-Ethyl-5-fluoro-1H-indole-2,3-dione 3-[4-(3-fluorophenyl) thiosemicarbazone] (7j)

Red powder (90%): mp 205–207 °C; IR (KBr): 3304, 3242 (NH), 1681 (C=O), 1273 (C=S). ^{1}H NMR (DMSO-d_6/ 400 MHz) ppm: 1.19 (3H, t, J: 7.2 Hz, indole N-CH_2CH_3), 3.78 (2H, q, J: 7.2 Hz, indole N-CH_2CH_3), 7.09–7.14 (1H, m, phenyl C_4-H), 7.22 (1H, dd, J: 8.7, 4.2 Hz, indole C_7-H), 7.29 (1H, td, J: 9.3, 2.2 Hz, indole C_6-H), 7.43–7.51 (2H, m, phenyl $C_{5,6}$-H), 7.62 (1H, dt, J: 10.9, 2.2 Hz, phenyl C_2-H), 7.67 (1H, dd, J: 8.0, 2.6 Hz, indole C_4-H), 10.88 (1H, s, N_4-H), 12.67 (1H, s, N_2-H). ^{13}C NMR (DECOUPLED DMSO-d_6/ 100 MHz): 12.99 (indole N-CH_2CH_3), 34.69 (indole N-CH_2CH_3), 108.87 (d, J: 26.1 Hz, indole C_4), 111.56 (d, J: 8.2 Hz, indole C_7), 112.57 (d, J: 24.8 Hz, phenyl C_2), 113.21 (d, J: 20.9 Hz, phenyl C_4), 117.96 (d, J: 24.1 Hz, indole C_6), 121.19 (d, J: 9.5 Hz, indole C_{3a}), 121.58 (d, J: 2.9 jHz, phenyl C_6), 130.41 (d, J: 9.3 Hz, phenyl C_5), 131.52 (d, J: 3.3 Hz, indole C_3), 139.41 (indole C_{7a}), 140.38 (d, J: 10.7 Hz, phenyl C_1), 159.04 (d, J: 238.3 Hz, indole C_5), 161.40 (indole C_2), 162.06 (d, J: 242.6 Hz, phenyl C_3), 176.51 (C=S). HRMS (ESI) $[M+H]^+$ $C_{17}H_{15}F_2N_4OS$: 361.09291; Found $[M+H]^+$: 361.09262. Anal. Calcd for $C_{17}H_{14}F_2N_4OS$: C, 56.66; H, 3.92; N, 15.55 Found: C, 56.62; H, 3.99; N, 15.63.

4.1.29. 1-Ethyl-5-fluoro-1H-indole-2,3-dione 3-[4-(4-fluorophenyl) thiosemicarbazone] (7k)

Orange powder (67%): mp 207–210 °C; IR (KBr): 3336, 3280, 3224 (NH), 1681 (C=O), 1271 (C=S). ^{1}H NMR (DMSO-d_6/ 400 MHz) ppm: 1.20 (3H, t, J: 7.2 Hz, N-CH_2CH_3), 3.80 (2H, q, J: 7.2 Hz, indole N-CH_2CH_3), 7.23–7.33 (4H, m, indole $C_{6,7}$-H, AA′BB′ system, phenyl $C_{3,5}$-H), 7.58–7.63 (2H, m, AA′BB′ system, phenyl $C_{2,6}$-H), 7.66 (1H, dd, J: 7.8, 2.6 Hz, indole C_4-H), 10.87 (1H, s, N_4-H), 12.63 (1H, s, N_2-H). ^{13}C NMR (DECOUPLED DMSO-d_6/ 100 MHz): 12.98 (indole N-CH_2CH_3), 34.69 (indole N-CH_2CH_3), 108.76 (d, J: 26.0 Hz, indole C_4), 111.52 (d, J: 8.1 Hz, indole C_7), 115.61 (d, J: 22.7 Hz, phenyl $C_{3,5}$), 117.85 (d, J: 24.1 Hz, indole C_6), 121.28 (d, J: 9.5 Hz, indole C_{3a}), 128.26 (d, J: 8.4 Hz, phenyl $C_{2,6}$), 131.27 (d, J: 3.3 Hz, indole C_3), 135.06 (d, J: 2.8 Hz, phenyl C_1), 139.34 (indole C_{7a}), 159.04 (d. J: 238.3 Hz. indole C_5), 160.50 (d. J: 243.3 Hz. phenyl C_4), 160.88 (indole C_2), 177.09 (C=S). HRMS (ESI) $[M+H]^+$ $C_{17}H_{15}F_2N_4OS$: 361.09291; Found $[M+H]^+$: 361.09280. Anal. Calcd for $C_{17}H_{14}F_2N_4OS$: C, 56.66; H, 3.92; N, 15.55 Found: C, 56.63; H, 4.02; N, 15.59.

4.1.30. 1-Ethyl-5-fluoro-1H-indole-2,3-dione 3-[4-(3-chlorophenyl) thiosemicarbazone] (7l)

Orange powder (95%): mp 194–197 °C; IR (KBr): υ 3304, 3197 (NH), 1681 (C=O), 1269 (C=S). ^{1}H NMR (DMSO-d_6/ 400 MHz) ppm: 1.20 (3H, t, J: 7.2 Hz, indole N-CH_2CH_3), 3.78 (2H, q, J: 7.2 Hz, indole N-CH_2CH_3), 7.22 (1H, dd, J: 8.6, 4.2 Hz, indole C_7-H), 7.28 (1H, td, J: 9.2, 2.7 Hz, indole C_6-H), 7.33 (1H, ddd, J: 8.1, 2.1, 1.0 Hz, phenyl C_4-H), 7.45 (1H, t, J: 8.1 Hz, phenyl C_5-H), 7.64–7.68 (2H, m, phenyl C_6-H, indole C_4-H), 7.78 (1H, t, J: 2.0 Hz, phenyl C_2-H), 10.89 (1H, s, N_4-H, D_2O exch), 12.67 (1H, s, N_2-H, D_2O exch). ^{13}C NMR (DECOUPLED $CDCl_3$/ 100 MHz): 12.70 (indole N-CH_2CH_3), 34.74 (indole N-CH_2CH_3), 108.45 (d, J: 25.7 Hz, indole C_4), 110.06 (d, J: 8.0 Hz, indole C_7), 117.79 (d, J: 24.3 Hz, indole C_6), 120.62 (d, J: 8.9 Hz, indole C_{3a}), 121.78 (phenyl C_6), 123.66 (phenyl C_2), 126.33 (phenyl C_4), 129.78 (phenyl C_5), 130.70 (d, J: 3.5 Hz, indole C_3), 134.42 (phenyl C_3), 138.65 (phenyl C_1), 138.94 (d, J: 2.0 Hz, indole C_{7a}), 159.32 (d, J: 242.3 Hz, indole C_5), 160.73 (indole C_2), 175.62 (C=S). LC/MS ESI $[M+H]^+$ $C_{17}H_{15}ClFN_4OS$: 377.84305; Found $[M+H]^+$: 377.5; 379.7. Anal. Calcd for $C_{17}H_{14}ClFN_4OS$: C, 54.18; H, 3.74; N, 14.87 Found: C, 53.69; H, 3.85; N, 14.48.

4.1.31. 1-Ethyl-5-fluoro-1H-indole-2,3-dione 3-[4-(4-chlorophenyl) thiosemicarbazone] (7m)

Orange powder (69%): mp 212–215 °C; IR (KBr): υ 3300, 3221 (NH), 1691 (C=O), 1271 (C=S). ^{1}H NMR (DMSO-d_6/ 400 MHz) ppm: 1.20 (3H, t, J: 7.2 Hz, indole N-CH_2CH_3), 3.79 (2H, q, J: 7.2 Hz, indole N-CH_2CH_3), 7.24 (1H, dd, J: 8.6, 4.2 Hz, indole C_7-H), 7.30 (1H, td, J: 8.8, 2.4 Hz, indole C_6-H), 7.49–7.52 (2H, m, AA′BB′ system, phenyl $C_{3,5}$-H), 7.65–7.68 (3H, m, AA′BB′ system, phenyl $C_{2,6}$-H, indole C_4-H)),

10.89 (1H, s, N_4-H), 12.67 (1H, s, N_2-H). ^{13}C NMR (DECOUPLED DMSO-d_6/ 100 MHz): 12.99 (indole N-CH_2CH_3), 34.68 (indole N-CH_2CH_3), 108.81 (d, J: 26.0 Hz, indole C_4), 111.56 (d, J: 8.1 Hz, indole C_7), 117.92 (d, J: 24.1 Hz, indole C_6), 121.22 (d, J: 9.5 Hz, indole C_{3a}), 127.61 (phenyl $C_{2,6}$), 128.81 (phenyl $C_{3,5}$), 130.66 (phenyl C_4), 131.44 (d, J: 3.3 Hz, indole C_3), 137.68 (phenyl C_1), 139.38 (indole C_{7a}), 159.03 (d, J: 238.3 Hz, indole C_5), 160.88 (indole C_2), 176.73 (C=S). HRMS (ESI) $[M+H]^+$ $C_{17}H_{15}ClFN_4OS$: 377.06336; 379.06041; Found: $[M+H]^+$: 377.06332; 379.06015. Anal. Calcd for $C_{17}H_{14}ClFN_4OS$: C, 54.18; H, 3.74; N, 14.87 Found: C, 53.63; H, 3.57; N, 15.30.

4.1.32. 1-Ethyl-5-fluoro-1H-indole-2,3-dione 3-[4-(4-bromophenyl) thiosemicarbazone] (7n)

Orange powder (79%): mp 213–216 °C; IR (KBr): υ 3300, 3226 (NH), 1689 (C=O), 1271 (C=S). ^{1}H NMR (DMSO-d_6/ 400 MHz) ppm: 1.20 (3H, t, J: 7.2 Hz, indole N-CH_2CH_3); 3.79 (2H, q, J: 7.2 Hz, indole N-CH_2CH_3); 7.24 (1H, dd, J: 8.4; 4.4 Hz, indole C_7-H); 7.30 (1H, td, J: 8.8; 2.4 Hz, indole C_6-H); 7.60–7.66 (4H, m, AA′BB′ system, phenyl$C_{2,3,5,6}$-H); 7.67 (1H, dd, J: 8.2; 2.6 Hz, indole C_4-H); 10.87 (1H, s, N_4-H); 12.67 (1H, s, N_2-H). ^{13}C NMR (DECOUPLED DMSO-d_6/ 100 MHz): 12.98 (indole N-CH_2CH_3), 34.70 (indole N-CH_2CH_3), 108.82 (d, *J:* 26.0 Hz, indole C_4), 111.57 (d, *J:* 8.1 Hz, indole C_7), 117.94 (d, *J:* 24.1 Hz, indole C_6), 118.93 (phenyl C_4), 121.23 (d, *J:* 9.5 Hz, indole C_{3a}), 127.86 (phenyl $C_{2,6}$), 131.47 (d, *J:* 3.3 Hz, indole C_3), 131.73 (phenyl $C_{3,5}$), 138.14 (phenyl C_1), 139.40 (indole C_{7a}), 159.05 (d, *J:* 238.3 Hz, indole C_5), 160.89 (indole C_2), 176.68 (C=S). HRMS (ESI) $[M+H]^+$ $C_{17}H_{15}BrFN_4OS$: 421.01285; 423.01080; Found $[M+H]^+$: 421.01276; 423.01053. Anal. Calcd for $C_{17}H_{14}BrFN_4OS$: C, 48.47; H, 3.35; N, 13.30 Found: C, 48.27; H, 3.17; N, 13.75.

4.2. Antiviral Activity

Antiviral effects of the compounds were determined using cytopathic effect (CPE) reduction assays. HEL cells were used to study HSV-1 strain KOS, a thymidine kinase-deficient (TK^-) HSV-1 KOS strain resistant to acyclovir, HSV-2 strain G and VV (Lederle strain). Vero cells were used for Coxsackie B4 virus [26,27].

The assays were performed in 96-well plates containing semiconfluent cell cultures. At the same time with the virus, serial dilutions of the test or reference compounds (brivudin, acyclovir and ganciclovir for HSV-1 and HSV-2 strains; DS-10.000, ribavirin and mycophenolic acid for Coxsackie B4 virus) were added. After the plates were incubated at 37 °C for 3–6 days, the antiviral activities [expressed as 50% effective concentration (EC_{50})] and cytotoxicity [expressed as minimum cytotoxic concentration (MCC)] of the compounds were determined by microscopy.

4.3. Molecular Modeling

4.3.1. Molecular Dynamics Simulations

Starting structures for molecular modeling were taken from rcsb protein data bank. For HSV-1 (gB) protein electron microscopy structure (PDB ID: 5fz2) [28] from strain KOS, for HSV-1 (gD) protein for HSV-1 (gD) protein X-ray diffraction structure (PDB ID: 1l2g, resolution: 2.85 Å) [29], and for HSV-2 (gD) protein X-ray diffraction structure (PDB ID: 3w9e, resolution: 2.3 Å) [30] from strain HG52, were obtained. HSV-1 (gB) and HSV-2 (gD) proteins were modeled as monomers, HSV-1 (gD) protein as dimer because of structural integrity between two monomers in the crystal structure.

All proteins were subjected to 10 ns long classical molecular dynamics (MD) simulations, utilizing GROMACS 5.0.0 program [31–33], which was utilized with GROMOS force field GROMOS96 54A7 [34]. Proteins were stripped off their water molecules and they were placed in truncated, rectangular boxes with dimensions of 8.0 × 8.0 × 14.0 nm and 8.0 × 8.0 × 10.0 nm, respectively. These dimensions ensured that at any point of the simulation the proteins stayed in the simulation box. The box was filled with single point charge (SPC) water molecules [35] and some of them were displaced during the addition of sodium and chloride ions to neutralize the system. At the beginning of simulations, starting systems were subsequently energy-minimized using the steepest descent method for 50,000 steps. Then, energy-minimized structures were taken for the production phase. MD simulations without any constraints were carried out using a constant number of particles (N), pressure (P), and temperature (T), i.e. NPT ensemble. The SETTLE algorithm was utilized to constrain the bond length and bond angle of the water molecules [36], while the LINCS algorithm was used to constrain the bond length of the peptide [37]. Long-range electrostatic interactions were calculated by particle-mesh Ewald (PME) method [38]. A constant pressure of 1 bar was applied with a coupling constant of 1.0 ps and water molecules/chloride ions were coupled separately to a bath at 303 K with a coupling constant of 0.1 ps. The equation of motion was integrated at 2 fs time steps using a leap-frog algorithm [39]. The tools available in the GROMACS and VMD 1.9.1. software [40] were utilized to analyze trajectories. Clustering tool of GROMACS (g_cluster) was used to obtain the most representative structures of 10 ns long trajectories.

Root mean square deviation (RMSD) values of all MD simulations showed that 10 ns long simulations were enough to equilibrate systems. With this methodology it was made sure that any structural anomalies and defects from x-ray and electron microscopy structures were overcome. Thus, average structures obtained for each protein were used to dock ligands in the next step, molecular docking simulations.

4.3.2. Molecular Docking Simulations

All docking simulations were performed utilizing AutoDock Vina 1.1.2 software [41]. Protein structures were put into a 3 × 3 × 3 nm grid box to occupy the whole ligand–protein systems and the spacing was kept at 1.00 Å, a standard value for AutoDock Vina. Each docking trial produced 20 poses with the exhaustiveness value of 20.

Structures of ligands were optimized by using YASARA software with YAMBER force field [42,43]. Binding poses were clustered and one binding pocket for each ligand, which produced the highest binding affinity, were assessed. Clustering criteria were bearing the highest binding affinity and the highest population of hits. Docking simulations for each ligand were repeated twice as AutoDock Vina uses a stochastic optimization algorithm. Repetition of simulations produced very similar binding results with very similar binding affinities.

Binding poses with the highest energies and more hits (number of poses, in which the ligands bind to the same binding site with different orientations) were identified as the best poses. Thus, for each ligand only the best poses were discussed.

Declaration of Competing Interest

The authors declare that they have no known competing financial interests or personal relationships that could have appeared to influence the work reported in this paper.

Acknowledgments

We thank Prof. Lieve Naesens from Rega Institute for Medical Research, Leuven, Belgium for antiviral screening of the compounds. This work was supported by Scientific and Technological Research Council of Turkey (TÜBİTAK) (grant number: 1003- 215S011).

Appendix A. Supplementary data

Supplementary data to this article can be found online at https://doi.org/10.1016/j.bioorg.2020.104202.

References and notes

[1] N. Terzioğlu, N. Karalı, A. Gürsoy, C. Pannecouque, P. Leysen, J. Paeshuyse, J. Neyts, E. De Clercq, Synthesis and primary antiviral activity evaluation of 3-hydrazono-5-nitro-2-indolinone derivatives, Arkivoc 1 (2006) 109–118, https://doi.org/10.3998/ark.5550190.0007.113.

[2] D. Banerjee, P. Yogeeswari, P. Bhat, A. Thomas, M. Srividya, D. Sriram, Novel isatinyl thiosemicarbazones derivatives as potential molecule to combat HIV-TB co-infection, Eur. J. Med. Chem. 46 (2011) 106–121, https://doi.org/10.1016/j.ejmech.2010.10.020.

[3] S.Y. Abbas, A.A. Farag, Y.A. Ammar, A.A. Atrees, A.F. Mohamed, A.A. El-Henawy, Synthesis, characterization, and antiviral activity of novel fluorinated isatin derivatives, Monatsh. Chem. 144 (2013) 1725–1733, https://doi.org/10.1007/s00706-013-1034-3.

[4] D.J. Bauer, P.W. Sadler, The structure-activity relationships of the antiviral chemotherapeutic activity of isatin β-thiosemicarbazone, Br. J. Pharmacol. 15 (1960) 101–110, https://doi.org/10.1111/j.1476-5381.1960.tb01216.x.

[5] J. Borysiewicz, W. Witaliński, Effect of N, N′-bis (methylisatin-β-thiosemicarbazone)-2-methylpiperazine on vaccinia virus replication *in vitro* and *in vivo*, Arch. Virol. 62 (1979) 83–86, https://doi.org/10.1007/BF01314907.

[6] A.J. Vyse, N.J. Gay, M.J. Slomka, R. Gopal, T. Gibbs, P. Morgan-Capner, D.W. Brown, The burden of infection with HSV-1 and HSV-2 in England and Wales: implications for the changing epidemiology of genital herpes, Sex. Transm. Infect. 76 (2000) 183–187, https://doi.org/10.1136/sti.76.3.183.

[7] H. Kaneko, T. Kawana, K. Ishioka, S. Ohno, K. Aoki, T. Suzutani, Evaluation of mixed infection cases with both herpes simplex virus types 1 and 2, J. Med. Virol. 80 (2008) 883–887, https://doi.org/10.1002/jmv.21154.

[8] I.J. Kang, L.W. Wang, T.A. Hsu, A. Yueh, C.C. Lee, Y.C. Lee, Y.S. Chao, S.R. Shih, J.H. Chern, Isatin-β-thiosemicarbazones as potent herpes simplex virus inhibitors, Bioorg. Med. Chem. Lett. 21 (2011) 1948–1952, https://doi.org/10.1016/j.bmcl.2011.02.037.

[9] S.S. Karki, A.A. Kulkarni, S. Kumar, S.K. Veliyath, E. De Clercq, J. Balzarini, Synthesis and biological evaluation of 2-(5-substituted-1-((diethylamino) methyl)-2-oxoindolin-3-ylidene)-N-substituted-hydrazinecarbothioamides, Med. Chem. Res. 22 (2013) 2014–2022, https://doi.org/10.1007/s00044-012-0184-x.

[10] Q. Zhong, Z. Yang, Y. Liu, H. Deng, H. Xiao, L. Shi, J. He, Antiviral activity of Arbidol against Coxsackie virus B5 in vitro and *in vivo*, Arch. Virol. 154 (2009) 601–607, https://doi.org/10.1007/s00705-009-0346-4.

[11] H. Akatsuka, Y. Yano, E.C. Gabazza, J. Morser, R. Sasaki, T. Suzuki, R. Fujiwara, A. Katsuki, Y. Takei, Y. Sumida, A case of fulminant type 1 diabetes with coxsackie B4 virus infection diagnosed by elevated serum levels of neutralizing antibody, Diabetes Res. Clin. Pract. 84 (2009) e50–e52, https://doi.org/10.1016/j.diabres.2009.03.009.

[12] N. Van der Werf, F.G.M. Kroese, J. Rozing, J.L. Hillebrands, Viral infections as potential triggers of type 1 diabetes, *Diabetes* Metab. Res. Rev. 23 (2007) 169–183, https://doi.org/10.1002/dmrr.695.

[13] F. Dotta, S. Censini, A.G.S. van Halteren, L. Marselli, M. Masini, S. Dionisi, F. Mosca, U. Boggi, A.O. Muda, S. Del Prato, J.F. Elliott, A. Covacci, R. Rappuoli, B.O. Roep, P. Marchetti, Coxsackie B4 virus infection of β cells and natural killer cell insulitis in recent-onset type 1 diabetic patients, Proc. Natl. Acad. Sci. U.S.A. 104 (2007) 5115–5120, https://doi.org/10.1073/pnas.0700442104.

[14] A. Karaküçük-İyidoğan, D. Taşdemir, E.E. Oruç-Emre, J. Balzarini, Novel platinum (II) and palladium (II) complexes of thiosemicarbazones derived from 5-substitutedthiophene-2-carboxaldehydes and their antiviral and cytotoxic activities, Eur. J. Med. Chem. 46 (2011) 5616–5624, https://doi.org/10.1016/j.ejmech.2011.09.031.

[15] A. Kolocouris, K. Dimas, C. Pannecouque, M. Witvrouw, G.B. Foscolos, G. Stamatiou, G. Fytas, G. Zoidis, N. Kolocouris, G. Andrei, R. Snoeck, E. De Clercq, New 2-(1-adamantylcarbonyl) pyridine and 1-acetyladamantane thiosemicarbazones–thiocarbonohydrazones: cell growth inhibitory, antiviral and antimicrobial activity evaluation, Bioorg. Med. Chem. Lett. 12 (2002) 723–727, https://doi.org/10.1016/S0960-894X(01)00838-1.

[16] Z. Atioğlu, Z.Ş. Sevinçli, N. Karalı, M. Akkurt, C.C. Ersanlı, 2-(5-Fluoro-1-methyl-2-oxoindolin-3-ylidene)-N-[4-(methylsulfanyl) phenyl] hydrazine-1-carbothioamide, IUCrData, 2 (2017), x170671. https://doi.org/10.1107/S241431461700671X.

[17] Z. Atioğlu, Z.Ş. Sevinçli, N. Karalı, M. Akkurt, C.C. Ersanlı, (2Z)-2-(5-Fluoro-1-methyl-2-oxoindolin-3-ylidene)-N-(3-fluorophenyl) hydrazine-1-carbothioamide, IUCrData 2 (2017) x170900, , https://doi.org/10.1107/S2414314617009002.

[18] S. Serra, L. Moineaux, C. Vancraeynest, B. Masereel, J. Wouters, L. Pochet, R. Frédérick, Thiosemicarbazide, a fragment with promising indolamine-2, 3-dioxygenase (IDO) inhibition properties, Eur. J. Med. Chem. 82 (2014) 96–105, https://doi.org/10.1016/j.ejmech.2014.05.044.

[19] E.B. Vasil'eva, D.V. Sevenard, O.G. Khomutov, O.A. Kuznetsova, Synthesis of trifluoroalkyl-and fluoroaryl-substituted 4,5-dihydro-1H-1,2,4-triazole-5-thiones, Russ. J. Org. Chem. 40 (2004) 874–878, https://doi.org/10.1023/B:RUJO.0000044552.07729.40.

[20] H. Huang, Q. Chen, X. Ku, L. Meng, L. Lin, X. Wang, C. Zhu, Y. Wang, Z. Chen, M. Li, H. Jiang, K. Chen, J. Ding, H. Liu, A series of α-heterocyclic carboxaldehyde thiosemicarbazones inhibit topoisomerase IIα catalytic activity, J. Med. Chem. 53 (2010) 3048–3064, https://doi.org/10.1021/jm9014394.

[21] S.K. Chawla, M. Arora, K. Nättinen, K. Rissanen, Unique copper ion catalyzed hydrolytic cleavage of C-N (2) bond of thiosemicarbazide, Polyhedron. 25 (2006) 627–634, https://doi.org/10.1016/j.poly.2005.05.021.

[22] S. Rádl, V. Zikán, V, Syntheses of some 4-dialkylaminoalkylamino derivatives of 2, 3-dimethyl-2H-and 3, 9-dimethyl-9H-pyrazolo [3, 4-b] quinoline, Collect. Czechoslov. Chem. Commun. 51 (1986) 1692–1697, https://doi.org/10.1135/cccc19861692.

[23] L.A. McAllister, R.A. McCormick, K.M. James, S. Brand, N. Willetts, D.J. Procter, A. Fluorous, Pummerer Cyclative-Capture Strategy for the Synthesis of N-Heterocycles, Chem. Eur. J. 13 (2007) 1032–1046, https://doi.org/10.1002/chem.200601429.

[24] X. Jia, Y. Zhu, Y. Yuan, X. Zhang, S. Lü, L. Zhang, L. Luo, C-H Activation Relay (CHAR): An Efficient Construction of Isatin Skeleton by Aerobic Oxidation of Glycine Esters, ACS Catal. 6 (2016) 6033–6036, https://doi.org/10.1021/acscatal.6b01781.

[25] H. Jiang, Q. Hu, J. Cai, Z. Cui, J. Zheng, W. Chen, Synthesis and dyeing properties of indophenine dyes for polyester fabrics, Dyes Pigm. 166 (2019) 130–139, https://doi.org/10.1016/j.dyepig.2019.03.025.

[26] L. Naesens, E. Vanderlinden, E. Roth, J. Jeko, G. Andrei, R. Snoeck, C. Pannecouque, E. Illyes, G. Batta, P. Herczegh, F. Sztaricskai, Anti-influenza virus activity and structure–activity relationship of aglycoristocetin derivatives with cyclobutenedione carrying hydrophobic chains, Antiviral Res. 82 (2009) 89–94, https://doi.org/10.1016/j.antiviral.2009.01.003.

[27] D. Rogolino, M. Carcelli, A. Bacchi, C. Compari, L. Contardi, E. Fisicaro, A. Gatti, M. Sechi, A. Stevaert, L. Naesens, A versatile salicyl hydrazonic ligand and its metal complexes as antiviral agents, J. Inorg. Biochem. 150 (2015) 9–17, https://doi.org/10.1016/j.jinorgbio.2015.05.013.

[28] T. Zeev-Ben-Mordehai, D. Vasishtan, A.H. Duran, B. Vollmer, P. White, A.P. Pandurangan, C.A. Siebert, M. Topf, K. Grunewald, Two distinct trimeric conformations of natively membrane-anchored full-length herpes simplex virus 1 glycoprotein B, Proc. Natl. Acad. Sci. USA 113 (2016) 4176–4181, https://doi.org/10.1073/pnas.1523234113.

[29] A. Carfi, S.H. Willis, J.C. Whitbeck, C. Krummenacher, G.H. Cohen, R.J. Eisenberg, D.C. Wiley, Herpes simplex virus glycoprotein D bound to the human receptor HveA, Mol. Cel. 8 (2001) 169–179, https://doi.org/10.1016/S1097-2765(01)00298-2.

[30] C.C. Lee, L.L. Lin, W.E. Chan, T.P. Ko, J.S. Lai, A.J. Wang, Structural basis for the antibody neutralization of herpes simplex virus, Acta Crystallogr D Biol Crystallogr. 69 (2013) 1935–1945, https://doi.org/10.1107/S0907444913016776.

[31] H.J.C. Berendsen, D. van der Spoel, R. van Drunen, GROMACS: a message-passing parallel molecular dynamics implementation, Comput. Phys. Commun. 91 (1995) 43–56, https://doi.org/10.1016/0010-4655(95)00042-E.

[32] E. Lindahl, B. Hess, D. van der Spoel, GROMACS 3.0: a package for molecular simulation and trajectory analysis, J. Mol. Model. 7 (2001) 306–317, https://doi.org/10.1007/s008940100045.

[33] D. Van Der Spoel, E. Lindahl, B. Hess, G. Groenhof, A.E. Mark, H.J.C. Berendsen, GROMACS: fast, flexible, and free, J. Comput. Chem. 26 (2005) 1701–1718, https://doi.org/10.1002/jcc.20291.

[34] N. Schmid, A.P. Eichenberger, A. Choutko, S. Riniker, M. Winger, A.E. Mark, W.F. van Gunsteren, Definition and testing of the GROMOS force-field versions 54A7 and 54B7, Eur. Biophys. J. 40 (2011) 843–856, https://doi.org/10.1007/s00249-011-0700-9.

[35] P.E. Smith, W.F. van Gunsteren, The viscosity of SPC and SPC/E water at 277 and 300 K, Chem. Phys. Lett. 215 (1993) 315–318, https://doi.org/10.1016/0009-2614(93)85720-9.

[36] S. Miyamoto, P.A. Kollman, Settle: An analytical version of the SHAKE and RATTLE algorithm for rigid water models, J. Comput. Chem. 13 (1992) 952–962, https://doi.org/10.1002/jcc.540130805.

[37] B. Hess, H. Bekker, H.J.C. Berendsen, J.G.E.M. Fraaije, LINCS: a linear constraint solver for molecular simulations, J. Comput. Chem. 18 (1997) 1463–1472, https://doi.org/10.1002/(SICI)1096-987X(199709)18:12<1463::AID-JCC4>3.0.CO;2-H.

[38] T. Darden, D. York, L. Pedersen, Particle mesh Ewald: An N· log (N) method for Ewald sums in large systems, J. Chem. Phys. 98 (1993) 10089–10092, https://doi.org/10.1063/1.464397.

[39] R.W. Hockney, S.P. Goel, J.W. Eastwood, Quiet high-resolution computer models of a plasma, J. Comput. Phys. 14 (1974) 148–158, https://doi.org/10.1016/0021-9991(74)90010-2.

[40] W. Humphrey, A. Dalke, K. Schulten, VMD: visual molecular dynamics, J. Molec. Graphics 14 (1996) 33–38, https://doi.org/10.1016/0263-7855(96)00018-5.

[41] O. Trott, A.J. Olson, AutoDock Vina: improving the speed and accuracy of docking with a new scoring function, efficient optimization, and multithreading, J. Comput. Chem. 31 (2010) 455–461, https://doi.org/10.1002/jcc.21334.

[42] E. Krieger, G. Vriend, Models@ Home: distributed computing in bioinformatics using a screensaver based approach, Bioinformatics 18 (2002) 315–318, https://doi.org/10.1093/bioinformatics/18.2.315.

[43] E. Krieger, T. Darden, S.B. Nabuurs, A. Finkelstein, G. Vriend, Making optimal use of empirical energy functions: force-field parameterization in crystal space, Proteins. 57 (2004) 678–683, https://doi.org/10.1002/prot.20251.